UNIVERSITATEA POLITEHNICA DIN BUCUREŞTI
FACULTATEA DE ŞTIINȚA ŞI INGINERIA MATERIALELOR
DEPARTAMENTUL: INGINERIA ŞI MANAGEMENTUL
OBŢINERII MATERIALELOR METALICE

PhD Thesis

STUDY AND COMPUTER THERMODYNAMIC ANALYSIS OF THE Bi-Sn ALLOY SYSTEM

STUDIUL ŞI ANALIZA TERMODINAMICĂ COMPUTERIZATĂ A SISTEMULUI DE ALIAJE Bi-Sn

Author: Eng. Emanuel-Laurenţiu NICULESCU

PhD supervisor: Prof.dr.eng. Mihai BUZATU

Bucharest, 2022

TABLE OF CONTENT

INTRODUCTION

There is currently a high market demand for lead-free and toxic-free solder alloys for use in electrical, electronic and other industrial fields. However, the development of new lead-free solder materials requires adequate thermophysical properties (properties related to their surface and the degree of wetting. Analyzing the specialized works in this field we found that Bi-Sn binary alloys are very often used in electrical engineering and electronics The Bi-Sn binary alloy must possesses physico-chemical characteristics specific to certain applications. Unfortunately, no thermodynamic data are known at certain working temperatures. Thus, the study of various processes in thermodynamics requires knowledge of the mechanism of phenomena that lead to those processes. Alloys of this type have a low melting temperature, which makes them suitable for soldering. Such light fusible alloys are frequently used in the automotive industry for the manufacture of small series of parts or unique series, having superior properties compared to pure alloy metals.

Because the thesis addresses "thermally" thermodynamic aspects from a theoretical point of view of easily fusible metallic materials such as Gibbs enthalpy, free enthalpy, entropy, thermodynamic activity, etc. this approach must be done within the specific conceptualization of physical metallurgy which has established itself as a distinct field. of the science of metallic materials. Thus, the phenomenology related to quantities: Gibbs enthalpy, free enthalpy, entropy, thermodynamic activity, etc. must be seen from the perspective of the structure of materials.

Keywords: ***Bi-Sn alloys, electrochemical cell; calculation and analysis of thermodynamic activities; measurement uncertainty***

1. THERMODYNAMICS OF Bi-Sn ALLOYS

1.1. PURPOSE AND OBJECTIVES OF THE THESIS

In recent years, many applications in the field of electronics have seen a rapid transition to a new type of alloy used for lead-free soldering. The main reason for rejecting materials used for lead solders is their toxicity. Environmental regulations around the world (European Union by restricting hazardous waste - RoHS and Waste Electrical and Electronic Equipment directives) aimed to eliminate the use of Pb-containing soldering materials and intensified research in this area.

1.2. PARTLY MOLAR THERMODYNAMIC FUNCTIONS FOR METAL MELT

$$Y = \sum_{i=1}^{n} n_i \overline{Y}_i \quad sau \quad dY = \sum_{i=1}^{n} d\overline{Y}_i n_i + \sum_{i=1}^{n} \overline{Y}_i dn_i \tag{1.1}$$

$$dY = \left(\frac{\partial Y}{\partial n_1}\right) dn_1 + \left(\frac{\partial Y}{\partial n_2}\right) dn_2 + \left(\frac{\partial Y}{\partial n_3}\right) dn_3 + \ldots\ldots\ldots + \left(\frac{\partial Y}{\partial n_n}\right) dn_n = \sum_{i=1}^{n} \overline{Y}_i dn_i \tag{1.2}$$

$$\sum_{i=1}^{n} d\overline{Y}_i n_i = 0 \tag{1.3}$$

$$\sum_{i=1}^{n} n_i d\overline{G}_i = 0 \; sau \sum_{i=1}^{n} n_i d\mu_i = 0 \tag{1.4}$$

$$\Delta\overline{G}_i = \mu_i - \mu_i^0 \tag{1.5}$$

$$\Delta\overline{Y}_i = \overline{Y}_i - Y_i^0 \tag{1.6}$$

$$\Delta\overline{G}_i = RT \ln \frac{p_i}{p_i^0} \tag{1.7}$$

$$\Delta\overline{G}_i = -z_i FE \tag{1.8}$$

$$x_1 \left(\frac{\partial \Delta\overline{Y}_1}{\partial x_2}\right) + x_2 \left(\frac{\partial \Delta\overline{Y}_2}{\partial x_2}\right) = 0 \tag{1.9}$$

$$\Delta\overline{G}_1(x_2) = -\int_0^{x_2} \frac{x_2}{1-x_2} \cdot \left(\frac{\partial \Delta\overline{G}_2}{\partial x_2}\right) dx_2 \tag{1.10}$$

$$\Delta\overline{G}_1(x_2) = -\int_0^{x_2} \frac{\Delta\overline{G}_2}{(1-x_2)^2} dx_2 - \frac{x_2 \Delta\overline{G}_2}{1-x_2} \tag{1.11}$$

$$\Delta Y^M = Y_m - \sum_{i=1}^{n} x_i Y_i^o \tag{1.12}$$

$$Y_m = \sum_{i=1}^{n} x_i \overline{Y}_i ; \left[Y_m = V_m, S_m, H_m, G_m\right] \tag{1.13}$$

$$\Delta Y^M = \sum_{i=1}^{n} x_i \overline{Y}_i ; \tag{1.14}$$

$$\Delta Y^M = x_1 \overline{Y}_1 + x_2 \overline{Y}_2 ; \tag{1.15}$$

$$\Delta\overline{Y}_2 = \Delta Y^M + (1-x_2)\left(\frac{\partial \Delta Y^M}{\partial x_2}\right) \tag{1.16}$$

$$\Delta Y^M = (1-x_2) \int_0^{x_2} \left(\frac{\Delta\overline{Y}_2}{(1-x_2)^2}\right) \tag{1.17}$$

1.2.1 THERMODYNAMIC MIXING FUNCTIONS

TEMPERATURE DEPENDENCE

$$G = H - TS \tag{1.18}$$

$$\Delta H^M = \Delta G^M + T\Delta S^M \tag{1.19}$$

$$\Delta S^M = (\Delta H^M - \Delta G^M)/T \tag{1.20}$$

$$\Delta \overline{H}_i = \Delta \overline{G}_i + T\Delta \overline{S}_i \tag{1.21}$$

$$\Delta \overline{S}_i = \frac{(\Delta \overline{H}_i - \Delta \overline{G}_i)}{T} \tag{1.22}$$

$$\frac{\partial \Delta G_i^T}{\partial T} = \left(\Delta \overline{G}_i - \Delta \overline{H}_i\right)\left(\frac{1}{T}\right) \tag{1.23}$$

$$\Delta \overline{H}_i = \Delta \overline{G}_i - T\frac{\partial \Delta \overline{G}_i}{\partial T} = -T^2\frac{\partial}{\partial T}\left(\frac{\partial \overline{G}_i}{T}\right) = \frac{\partial\left(\Delta \overline{G}_i / T\right)}{\partial(1/T)} \tag{1.24}$$

$$\Delta \overline{H}_i = -RT^2\left(\partial \ln a_i / \partial T\right) = -RT^2\left(\partial \ln \gamma_i / \partial T\right) = RT\ln\gamma_i - T\frac{\partial}{\partial T}\left(RT\ln\gamma_i\right) = \Delta \overline{G}_i^E - T\left(\partial \Delta G_i^E / \partial T\right) \tag{1.25}$$

$$\Delta \overline{G}_i = RT\ln a_i = RT\ln x_i + RT\ln\gamma_i \tag{1.26}$$

$$\Delta \overline{S}_i = -\frac{\partial \Delta \overline{G}_i}{\partial T} = -R\ln x_i - \frac{\partial}{\partial T}\left(RT\ln\gamma_i\right) = -R\ln x_i - \frac{\partial \Delta \overline{G}_i^E}{\partial T} \tag{1.27}$$

$$\Delta \overline{S}_i = -\frac{\partial \Delta \overline{G}_i}{\partial T} = -\frac{\partial (z_i FE)}{\partial T} = z_i F\frac{\partial E}{\partial T} \tag{1.28}$$

$$\Delta \overline{S}_i(ideal) = -R\ln x_i \tag{1.29}$$

1.3. EXCESS THERMODYNAMIC FUNCTIONS

$$\Delta \overline{Y}_i^E = \Delta \overline{Y}_i - \Delta \overline{Y}_i^{id} \tag{1.30}$$

$$\Delta \overline{Y}_i^E = \Delta \overline{Y}_i - \Delta \overline{Y}_i^{id} \tag{1.31}$$

$$\Delta \overline{G}_i^E = \Delta \overline{G}_i^M - RT\ln x_i = RT\ln\gamma_i \tag{1.32}$$

$$\Delta \overline{S}_i^E = \Delta \overline{S}_i^M - (-R\ln x_i) = \Delta \overline{S}_i^M + R\ln\gamma_i \tag{1.33}$$

$$\Delta \overline{H}_i^{id} = 0 \; si \; \Delta \overline{V}_i^{id} = 0 \Rightarrow \Delta \overline{H}_i^E = \Delta \overline{H}_i^M ; \Delta \overline{V}_i^E = \Delta \overline{V}_i^M \tag{1.34}$$

$$\Delta \overline{Y}_i^E = \Delta Y^E + (1 - x_i)\left(\frac{\partial \Delta Y^E}{\partial x_i}\right) \tag{1.35}$$

$$\Delta Y^E = (1 - x_2)\int_0^{x_2} \frac{\Delta \overline{Y}_2^E}{(1 - x_2)^2} dx_2 \tag{1.36}$$

2. DETERMINATION OF THERMODYNAMIC ACTIVITY BASED ON MEASUREMENT OF ELECTROMOTIVE VOLTAGE

The method is based on measuring the electromotive voltage in a cell of reversible concentration using solid or liquid electrolyte. By definition, electrochemical systems in which electrodes differ only in the activity (concentration) of the components are called concentration cells. In a cell of this type the energy source is the transfer energy from the higher activity substance to the lower activity substance.

Solid type electrolyte cells

This method consists in measuring the electromotive voltage of such an electrochemical chain:

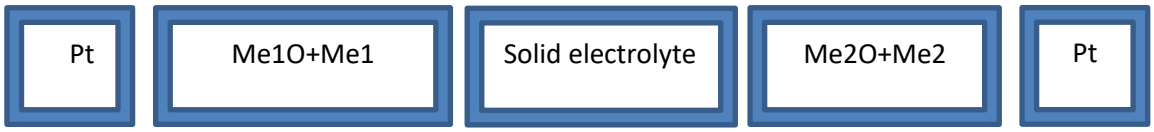

3. ESTIMATION OF MEASUREMENT UNCERTAINTY

The result of a measurement, after correction for the identified systematic effects, remains only an estimate of the value of the measurand, this being due to the ignorance of the random effects and due to the imperfect correction of the result for the systematic effects (eliminated).

3.1. MEASUREMENT (BASIC CONCEPTS)

Measurement is a cumulation of operations by how to determine the value of the desired size.It is necessary that the measurement starts with the correct definition of the measurand and the method of measurement, materialized by a measurement procedure.

3.2 CLASSIFICATION OF MEASUREMENT ERRORS

Classification of errors according to the mode of representation:
a) Absolute error, Δ
b) Relative error
c) Reported error
d) Tolerated error.

3.3. UNCERTAINTY ASSESSMENT

According to the relation $x = a + D + \varepsilon_a$, the uncertainties associated with the two effects must be estimated: the random one and the systematic one.

3.4. NUMERICAL CALCULATION METHODS

3.4.1. SIMPSON METHOD

In this method, the formula for calculating the approximate value of the integral, which is obtained by approximating the function f by a Lagrange polynomial of degree two at most two, which interpolates the function f.

3.4.2. METHOD OF THE TRAPEZ

This method is obtained by approximating the function to be integrated with a Lagrange interpolation polynomial constructed on nodes a and b, i.e. by a first degree Lagrange polynomial.

x	a	b
f	f(a)=f1	f(b)=f2

3.5 CURRENT STATE OF Sn-Bi ALLOYS USED TO CONTACT ELECTRONIC COMPONENTS

The thesis addresses the Bi-Sn alloy system that are used in the electronics industry in Romania and around the world. The topic of this doctoral thesis is relevant due to the scientific and technological content assimilated and developed as well as through the practical applicability of the studied materials. The scientific content seen through the prism of the subjects in the field of physics, chemistry, materials science and mathematical and computational instrumentation is important for the entire doctoral thesis and therefore in the following will be a brief presentation of the applicability of alloys in the Bi-Sn system. mainly in the conventional and industrial electronics industry. Among them, the soldering alloys in the Sn-Bi system proved to be superior for several reasons, such as lower melting temperature, good tensile strength, good reliability and creep resistance. At the same time, the cost of Sn-Bi soldering is lower than others. However, two main problems limiting the application of Sn-Bi base solders in electronic assembly are the brittleness and poor ductility of Sn-Bi alloys.

3.5.1 PHYSICO-CHEMICAL PROPERTIES OF Bi

The chemical element, Bi, is found in group I5 (V A) of the periodic table; having the atomic number Z = 83 and its atomic mass is 208.98 um. In its pure state bismuth can be found in nature either combined; bismuth (bismuth sulfide, Bi2S3) being one of the most important ores. Bismuth has a reddish-white color and is a brittle material. This metal shows a strong diamagnetism. The thermal conductivity of bismuth is the lowest, only mercury exceeds it at this value.

3.5.2 PHYSICO-CHEMICAL PROPERTIES OF Sn

Tin is found in nature mainly in the form of cassiterite (tin dioxide, SnO_2) in granite rocks, along with quartz, iron ores, copper and lead. For the extraction of tin, the cassiterite must first undergo an enrichment operation, until the concentration in SnO_2 increases up to 60%. It is a metal known since ancient times. Tin is a 4th group metal in the periodic table of elements. It is obtained mainly from the mineral cassiterite, which contains tin oxide, SnO.

3.6 ALLOYS FOR ELECTRONIC CONTACT OR WELDING ALLOYS

Solder alloys must have low melting temperature, good wetting properties, diffusion capacity, high fluidity, good corrosion resistance, etc. In addition to the very good adhesion and the lowest possible contact resistance to the metals subjected to soldering, these alloys must be inert to corrosion agents and have high electrical conductivity when used when soldering electrical conductors. .

The most used solder alloys in electronics are those in the systems: Sn-Pb; Sn-Pb-Cd; Sn-Pb-Zn. In the tin - lead system the two metals are totally miscible in liquid state, and in solid state the maximum solubility corresponds to the eutectic temperature of 183^0C at which the solubility of tin in lead is 19.2%, and of lead in tin of 2.5%.

3.7 MECHANICAL PROPERTIES OF Sn-Bi ALLOYS

Practice has shown that Sn-Bi base solders exhibit brittle behavior that can be fatal to electronic products. But the tensile strength and shear strength of Sn-Bi-based solders is superior to those based on Sn-Pb. Sn-Bi-based solder joints are more reliable than many other types of solder joints. However, Sn-Bi base solders are not the best when compared to the mechanical properties of lead-free solder joints. In order to improve the mechanical properties of the Sn-Bi base welds, trace level elements were added to the base alloy in order to refine the weld microstructures. Shen et al. reported that the average tensile strength of Sn-58Bi solder is 73.24 MPa.

3.8 ELECTROMIGRATION IN THE Sn-Bi SYSTEM MAJOR PROBLEM A SOLDER RELIABILITY

Electromigration is defined as atomic diffusion caused by an intense electric current. The electronics industry aims to use high densities of electricity. High current densities can cause some defects in the solder joints. Electromigration also affects the formation of compounds at the interface between the solder alloy and the PAD, such as coarse granulation and mass accumulation of Bi in the solder.

4. METHODS FOR DETERMINING THERMODYNAMIC MEASURES

4.1. EMPIRICAL METHODS

The dependence of the thermodynamic properties on the state parameters cannot be established theoretically, with sufficient precision, for this reason the formal description of these properties based on empirical relationships

4.2. THEORETICAL METHODS

SUBSUBREGULAR SOLUTION MODEL

The difference between the subregular solution model and the subregular solution model is given by the presence of additional interaction energy between type 1 and type 2 atoms. And in the case of the subsubregular solutions model, the solution is considered disordered entropy of mixture having the same expression as in the case of ideal solutions.

5. EXPERIMENTAL RESEARCH METHOD

In this research paper on the thermodynamics of Bi-Sn binary alloys, we considered the method of measuring electromotive voltage a safe, reproducible and accurate method. This method consists in measuring the electromotive voltage of the molten metal in a galvanic cell of reversible concentration with solid electrolyte. The main source of energy in this type of cell is the transfer energy from a substance that has a higher thermodynamic activity to a substance with a much lower thermodynamic activity.

The schematic representation of this galvanic cell is shown below:

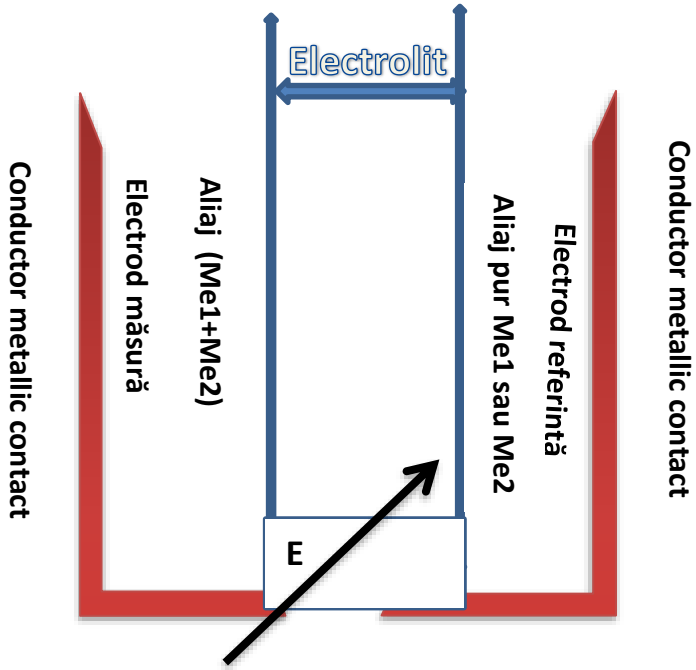

Figure 5.1. Schematic representation of the galvanic cell

$$\Delta\bar{G} = -zEF \quad (5.1)$$

$$\Delta\bar{G}_{Bi} = RTln\, a_{Bi} = RTln\gamma_{Bi} + RTlnx_{Bi} \quad (5.2)$$

$$\Delta\bar{G}_{Sn} = RTlna_{Sn} = RTln\gamma_{Sn} + RTlnx_{Sn} \quad (5.3)$$

$$x_{Bi}\frac{\partial lna_{Bi}}{\partial x_{Sn}} + x_{Sn}\frac{\partial lna_{Sn}}{\partial x_{Bi}} = 0 \quad (5.4)$$

$$x_{Bi}\frac{\partial ln\gamma_{Bi}}{\partial x_{Sn}} + x_{Sn}\frac{\partial n\gamma_{Sn}}{\partial x_{Bi}} = 0 \quad (5.5)$$

$$lna_{Sn} = -\int_0^{x_{Bi}} \frac{x_{Bi}}{1-x_{Bi}}\frac{\partial lna_{Bi}}{\partial x_{Bi}}dx_{Bi} = \int_0^{x_{Bi}} \frac{lna_{Bi}}{(1-x_{Bi})^2}dx_{Bi} - \frac{x_{Bi}}{1-x_{Bi}}lna_{Bi} \quad (5.6)$$

$$ln\gamma_{Sn} = -\int_0^{x_{Bi}} \frac{x_{Bi}}{1-x_{Bi}}\frac{\partial ln\gamma_{Bi}}{\partial x_{Bi}}dx_{Bi} = \int_0^{x_{Bi}} \frac{ln\gamma_{Bi}}{(1-x_{Bi})^2}dx_{Bi} - \frac{x_{Bi}}{1-x_{Bi}}ln\gamma_{Bi} \quad (5.7)$$

5.1. EXPERIMENTAL INSTALLATION

In order to be able to calculate the thermodynamic activity of the Bi-Sn system, we used the galvanic cell of reversible concentration in which we used as a measuring electrode the Bi-Sn alloy with various chemical compositions. Pure Bi was used for the reference electrode. Bi and Sn metals were purchased from Alfa Aesar Co., and as electrolyte we used a mixture of salts from the KCl - NaCl - $PbCl_2$ system whose chemical composition, in molar percentages, was: 35% KCl, 17% NaCl and 48% $PbCl_2$, the melting temperature of the electrolyte being 399°C (672 K), according to the electrochemical chain:

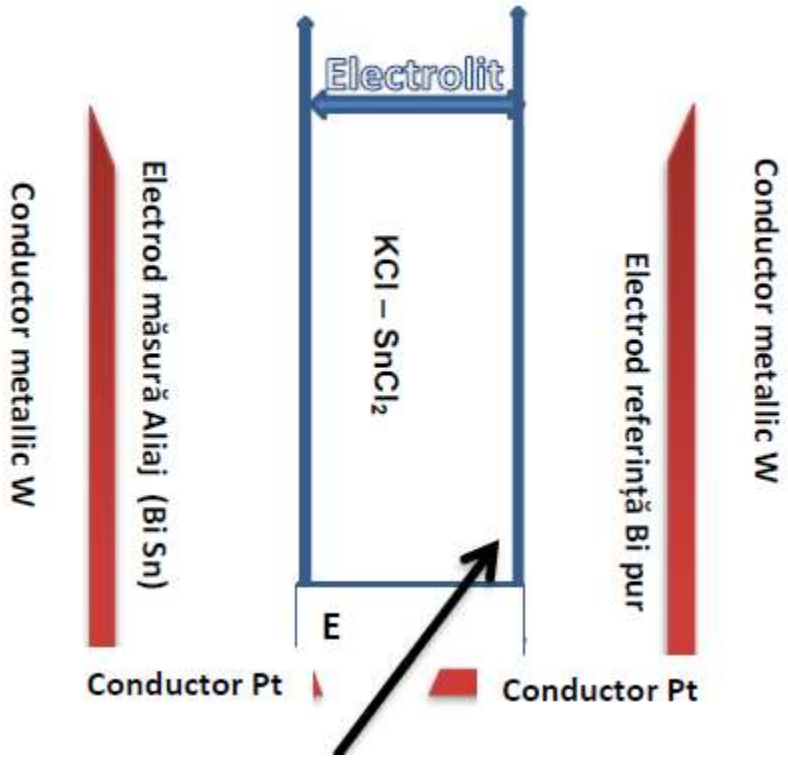

Figure 5.2 Galvanic concentration cell scheme

6. EXPERIMENTAL RESULTS AND THEIR INTERPRETATION

6.1 DETERMINATION OF THERMODYNAMIC FUNCTIONS BY METHOD OF MEASURING ELECTROMOTIVE VOLTAGE AT 600K

Table 6.1

Measured values, average values of electromotive voltages at 600K and 903K and statistical parameters of uncertainty

EMF (mV)	EMF Electric motor voltage (mV)									
	0,1	0,2	0,3	0,4	0,5	0,6	0,7	0,8	0,9	1
600K										
E_1	35,712	24,553	18,953	14,821	11,533	8,481	5,961	3,668	1,654	0,005
E	34,621	23,951	19,007	14,913	11,392	7,953	6,256	3,991	1,534	0,005
E_3	36,803	24,95	18,903	14,906	11,381	8,452	5,784	3,227	1,88	0,008
E_4	35,708	24,952	18,952	14,521	11,444	8,48	5,833	3,765	1,499	0,002
E_5	35,712	24,954	18,951	14,63	11,332	8,453	5,99	3,757	1,672	0,005
$\overline{E}$	35,7	24,7	18,95	14,8	11,4	8,4	6,0	3,7	1,7	0,005
SD	0,8	0,4	0,04	0,2	0,1	0,2	0,2	0,3	0,1	0,002
RSD (%)	2,2	1,8	0,2	1,2	0,7	2,7	3,1	7,6	8,8	42,4
903K										
E_1	31,423	23,902	18,124	13,705	9,523	6,112	3,532	1,802	0,802	0,009
E_2	31,415	23,713	18,703	13,621	9,904	6,218	3,712	1,666	0,276	0,008
E_3	31,502	23,806	18,421	13,704	9,565	6,217	3,564	1,706	0,648	0,009
E_4	31,203	23,721	18,231	13,617	9,902	6,203	3,703	1,812	0,721	0,009
E_5	31,516	23,903	18,636	13,803	9,736	6,133	3,71	1,665	0,336	0,009
$\overline{E}$	31,4	23,8	18,4	13,7	9,7	6,2	3,6	1,7	0,6	0,0088
SD	0,1	0,1	0,3	0,1	0,2	0,1	0,1	0,1	0,2	0,0004
RSD (%)	0,4	0,4	1,4	0,6	1,9	0,8	2,4	4,2	42,4	5,1

6.1.1 DETERMINATION OF THERMODYNAMIC ACTIVITIES

Table 6.2

Bi thermodynamic activity at 600K

Molar fraction	1	0,9	0,8	0,7	0,6	0,5	0,4	0,3	0,2	0,1	0,0
1.aBi	1	0,902	0,806	0,712	0,617	0,52	0,425	0,329	0,23	0,123	0,0
2. aBi	1	0,900	0,802	0,706	0,613	0,519	0,426	0,331	0,232	0,124	0,0

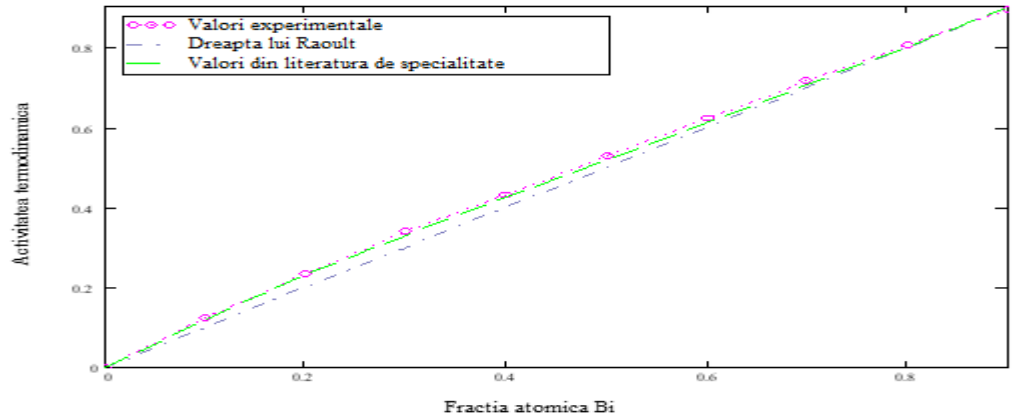

Figure 6.1.Variation of the thermodynamic activity of Bi depending on the atomic fraction in the binary alloy Bi-Sn at 600K experimental values and values from the literature

Table 6.3

Thermodynamic activity Sn at 600K

Molar fraction	1	0,9	0,8	0,7	0,6	0,5	0,4	0,3	0,2	0,1	0,0
1.aSn	1	0,903	0,806	0,715	0,620	0,525	0,428	0,329	0,225	0,116	0,0
2.aSn	1	0,904	0,813	0,723	0,632	0,537	0,439	0,337	0,229	0,116	0,0

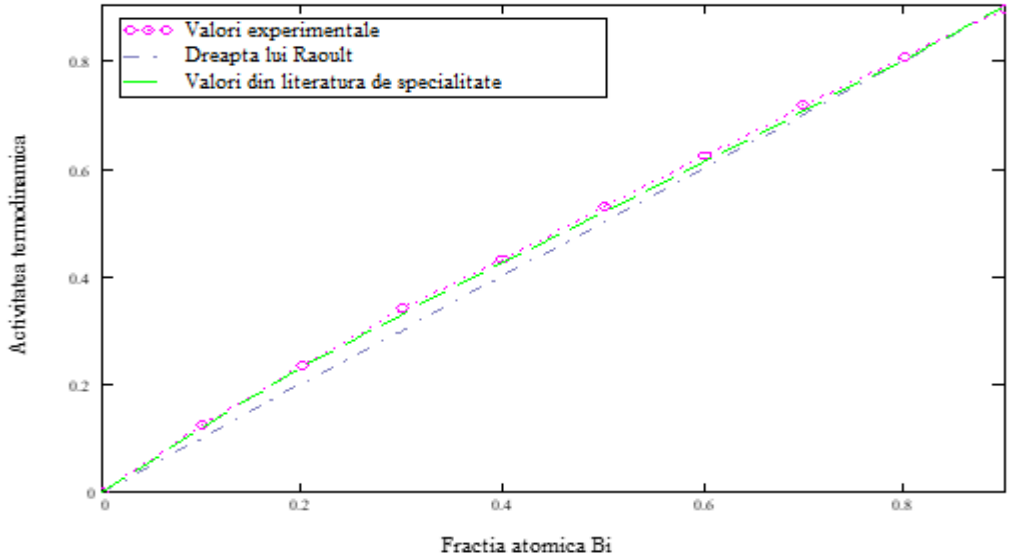

Figura 6.2 Variation of the thermodynamic activity of Sn depending on the atomic fraction in the binary alloy Bi-Sn at 600K experimental values and values from the literature

6.1.2 DETERMINATION OF THERMODYNAMIC ACTIVITY COEFFICIENTS

Table 6.4

Coefficients of thermodynamic activity of Bi at 600K

Molar fraction	1	0,9	0,8	0,7	0,6	0,5	0,4	0,3	0,2	0,1	0,0
1.ϒBi	1	1,0018	1,008	1,017	1,030	1,051	1,076	1,121	1,174	1,253	1,31
2ϒBi	1	1,000	1,002	1,009	1,021	1,039	1,065	1,104	1,160	1,241	1,356

Table 6.5

Coefficients of thermodynamic activity of Sn at 600K

Molar fraction	1	0,9	0,8	0,7	0,6	0,5	0,4	0,3	0,2	0,1	0,0
1.ϒSn	1	1,003	1,010	1,021	1,033	1,051	1,069	1,096	1,126	1,156	1,161
2ϒSn	1	1,004	1,016	1,033	1,053	1,075	1,097	1,122	1,145	1,159	1,158

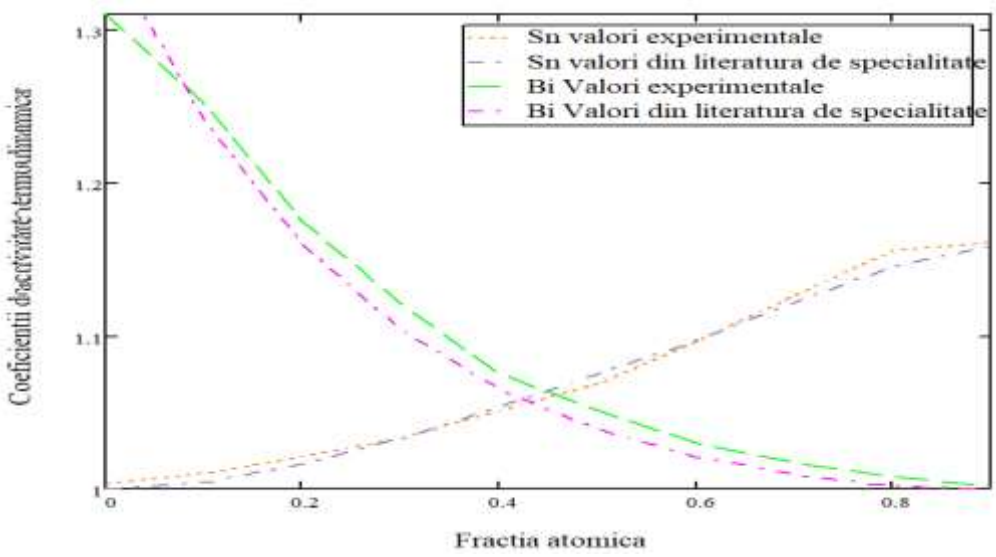

Figure 6.3 Variation of thermodynamic activity coefficients for Bi and Sn depending on the atomic fraction in the Bi-Sn binary alloy at 600K experimental values and values calculated based on data from the literature

6.1.3 DETERMINATION OF PARTIALLY MOLAR FREE ENERGIES OF EXCESS

Table 6.6

Partially molar free energies of excess for Bi at 600K

Molar fraction	1	0,9	0,8	0,7	0,6	0,5	0,4	0,3	0,2	0,1	0,0
1..$\Delta\bar{G}eBi[J/mol]$	0	8,971	39,748	84,9	147,451	248,133	365,403	569,781	800,223	1125	+∞
2.$\Delta\bar{G}eBi[J/mol]$	0	9,967	44,695	103,672	190,85	314,143	493,552	740,378	1077	1519	+∞

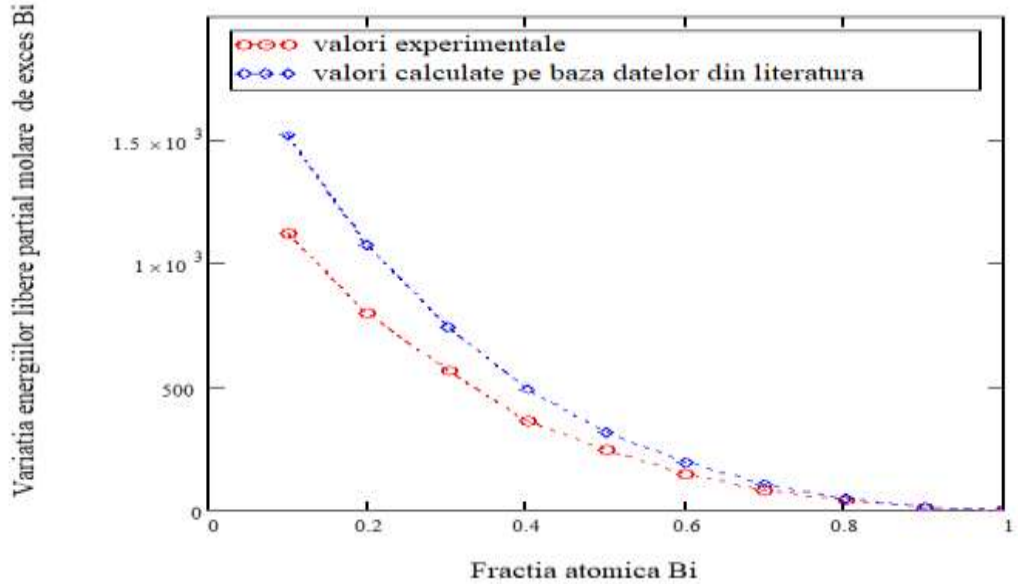

Figure 6.4 Partially excess molar free energy values for Bi as a function of the atomic fraction in the Bi-Sn binary alloy at 600K experimental values and values calculated based on the values in the literature

Table 6.7

Partially molar free energies of excess for Sn at 600K

Molar fraction	1	0,9	0,8	0,7	0,6	0,5	0,4	0,3	0,2	0,1	0
1.$\Delta\bar{G}eSn[J/mol]$	0	14,943	49,636	103,672	161,959	248,133	332,844	457,273	591,98	723,174	+∞
2.$\Delta\bar{G}eSn[J/mol]$	0	19,914	79,183	161,959	257,617	360,764	461,822	574,229	675,45	731,77	+∞

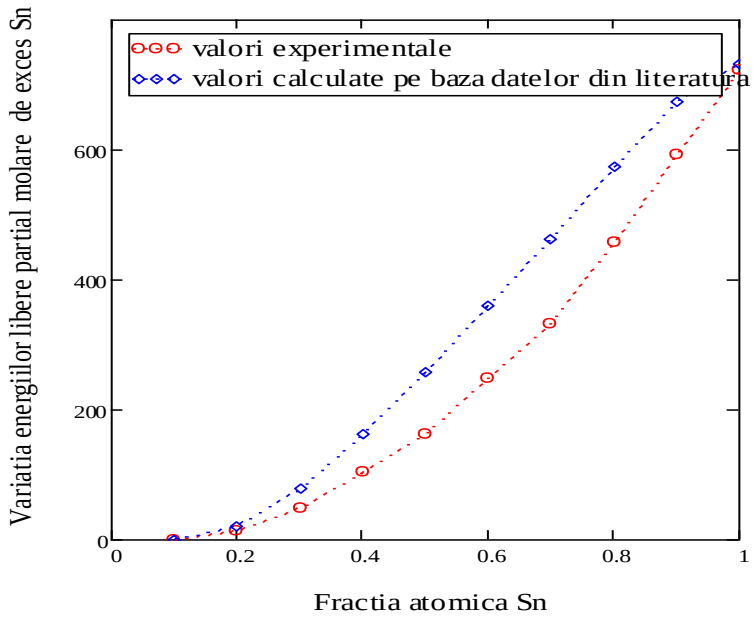

Figure 6.5 Partially excess molar free energy values for Sn as a function of Sn atomic fraction in Bi-Sn binary alloy at 600K experimental values and values calculated from the values in the literature

Table 6.8

Partially molar free energies Bi at 600K

Molar fraction	1	0,9	0,8	0,7	0,6	0,5	0,4	0,3	0,2	0,1	0,0
1..$\Delta\bar{G}Bi$ [J/mol]	0	-547,8	-1070	-1667	-2370	-3186	-4210	-5396	-7224	-10370	-∞
2.$\Delta\bar{G}Bi$ [J/mol]	0	-525,58	-1101	-1737	-2441	-3272	-4257	-5515	-7288	-10580	-∞

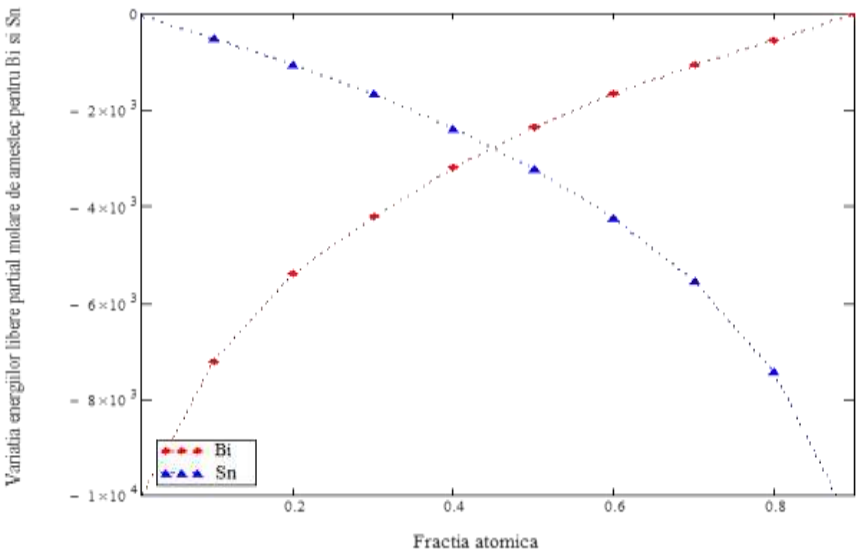

Figure 6.6 Partially molar free energy values at 600K for Bi and Sn, experimental values

Table 6.8

Partially molar free energies Sn at 600K

Molar fraction	1	0,9	0,8	0,7	0,6	0,5	0,4	0,3	0,2	0,1	0
1.$\Delta\bar{G}Sn$ *[J/mol]*	0	-508,98	-1063	-1673	-2385	-3214	-4233	-5546	-7441	-10750	-∞
2.$\Delta\bar{G}Sn$ *[J/mol]*	0	-503,459	-1033	-1618	-2289	-3102	-4107	-5426	-7353	-10750	-∞

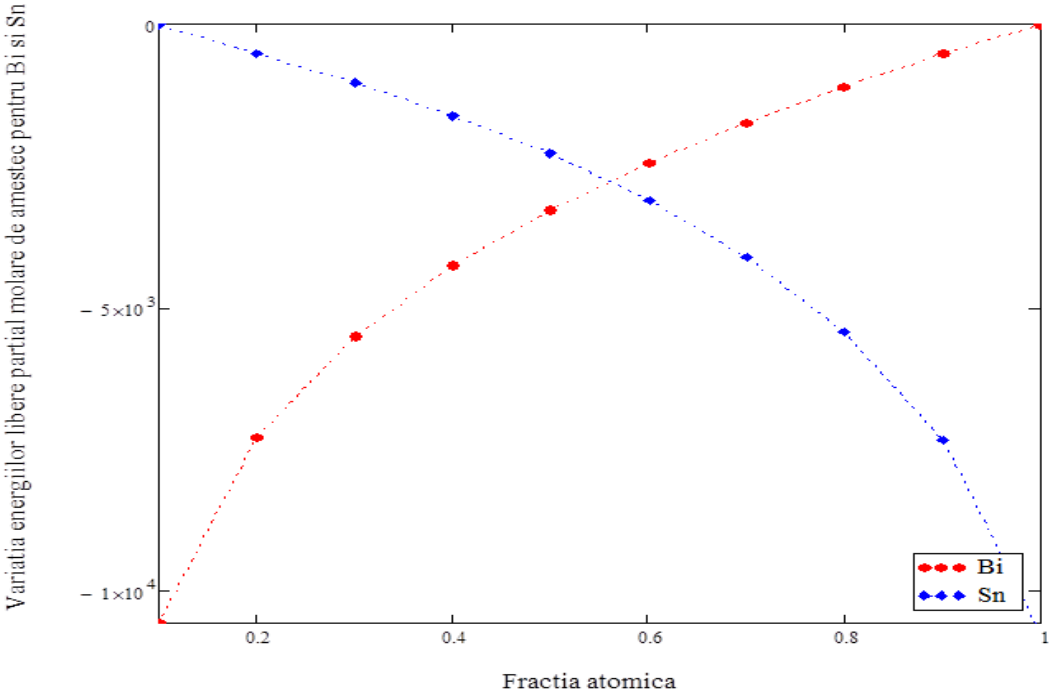

Figure .6.7 Partially molar free energy values at 600K for Bi and Sn, values calculated based on data from the literature

Table 6.10

Interaction parameters for Bi at 600K

Molar fraction	1	0,9	0,8	0,7	0,6	0,5	0,4	0,3	0,2	0,1	0
1.$\omega Bi[J/mol]$	0	88,710	198,740	283,000	368,627	496,266	609,005	813,973	1100	1250	$+\infty$
2.$\omega Bi[J/mol]$	0	99,670	223,475	345,573	477,125	628,286	822,587	1058	1346	1688	$+\infty$

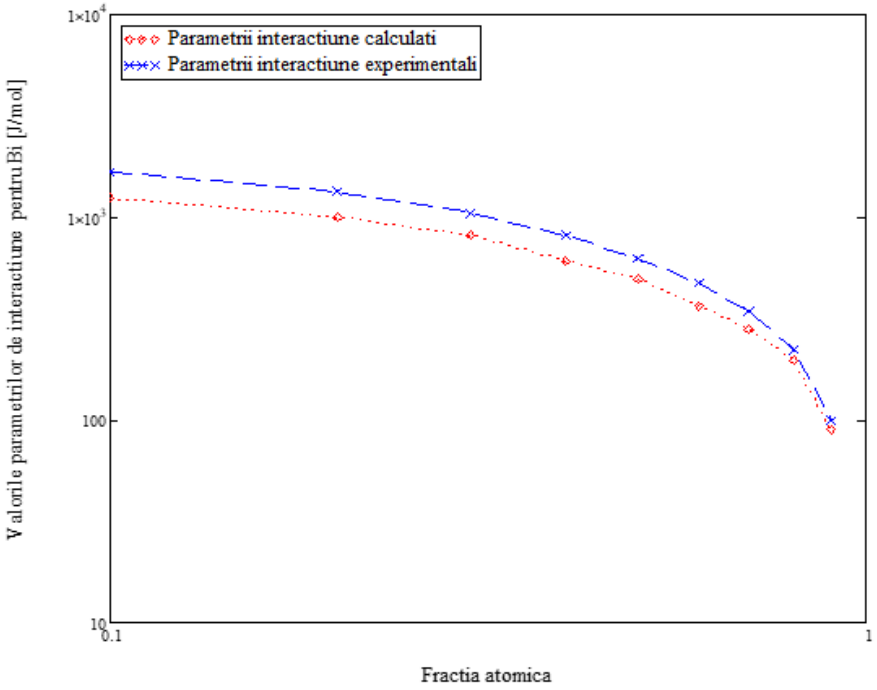

Figure.6.8 Variations of interaction parameters at 600K temperature for Bi, values calculated based on data from the literature and experimental values.

Table 6.11

Interaction parameters for Sn at 600K

Molar fraction	1	0,9	0,8	0,7	0,6	0,5	0,4	0,3	0,2	0,1	0
1.$\omega Sn[J/mol]$	0	149,430	248,180	345,573	404,897	496,266	554,740	653,247	739,975	803,527	$+\infty$
2.$\omega Sn[J/mol]$	0	199,140	395,915	539,863	644,043	721,528	769,703	820,327	844,313	898,725	$+\infty$

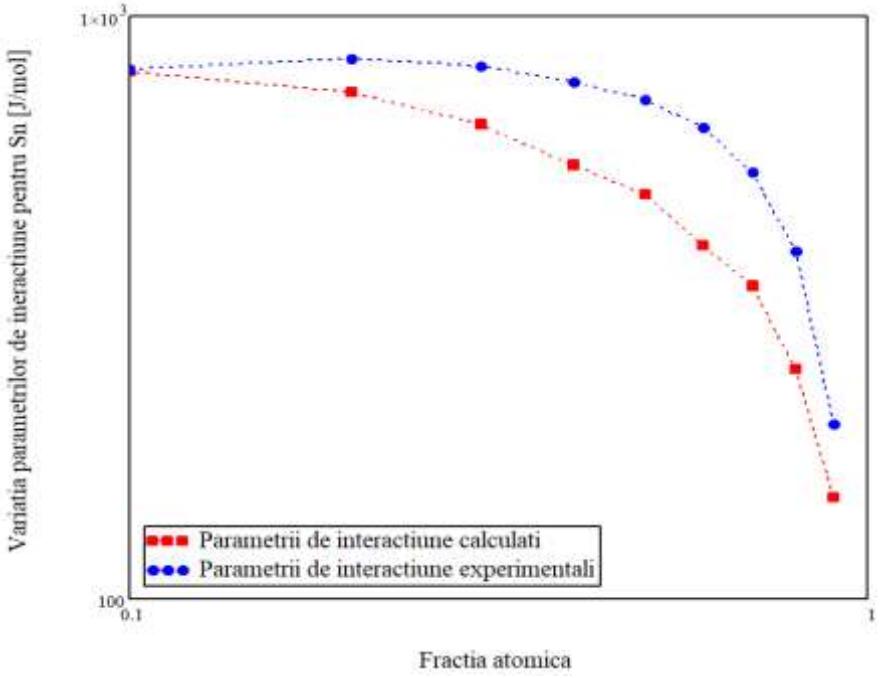

Figure.6.9 Variations of interaction parameters at 600K temperature for Sn, values calculated based on data from the literature and experimental values.

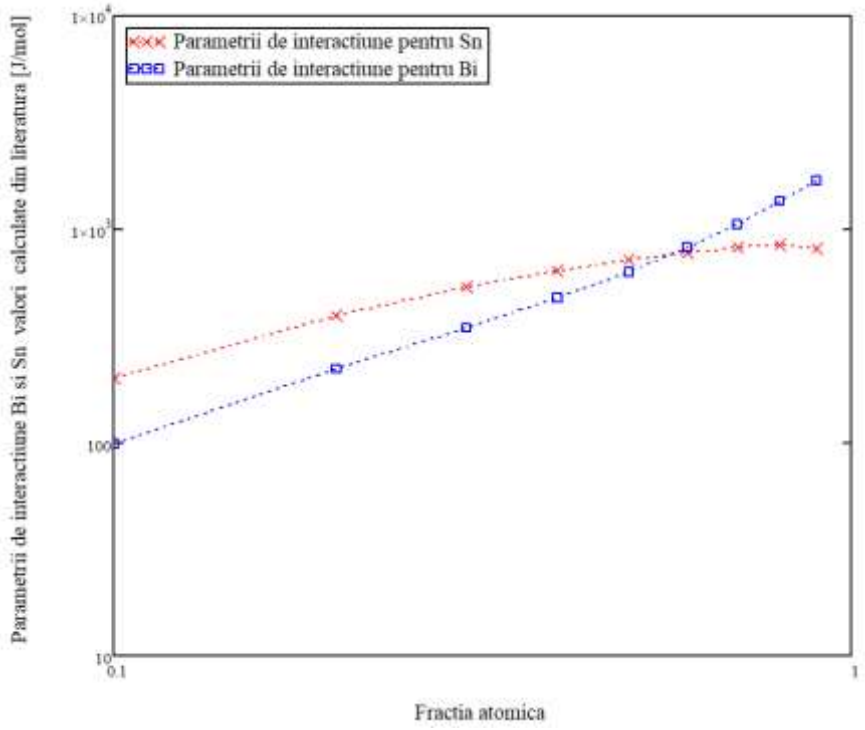

Figure.6.10 Variations of interaction parameters at 600K temperature for Sn and Bi, values calculated based on data from the literature

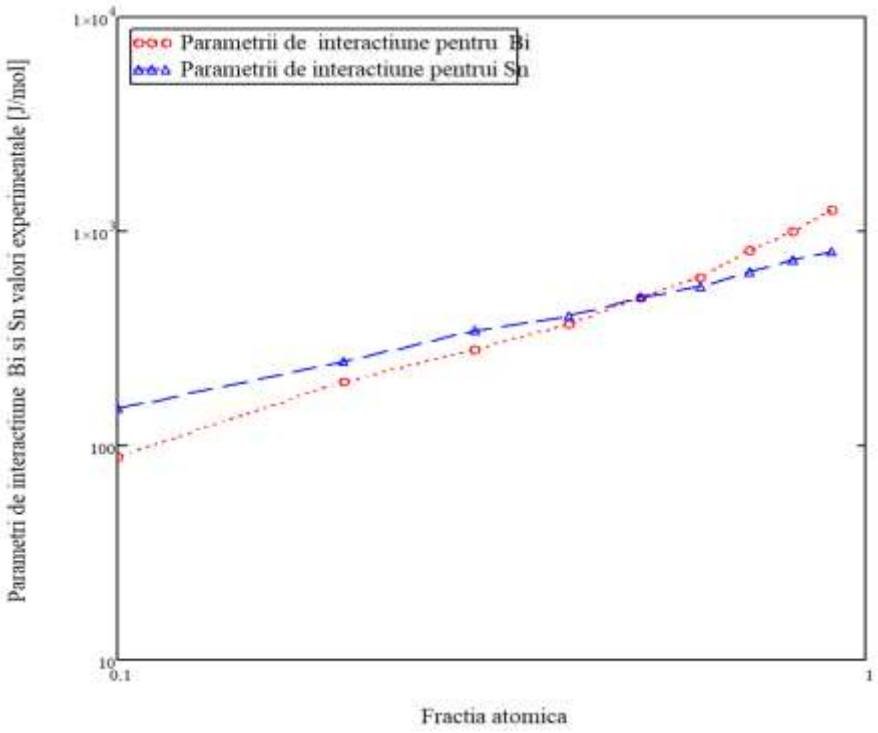

Figure.6.11 Variations of interaction parameters at 600K temperature for Sn, values calculated based on experimental data.

6.2. BINARY THERMODYNAMIC CALCULATION (CTB)

The CTB program was created using the JAVA programming language.

6.3. DETERMINATION OF THERMODYNAMIC FUNCTIONS AT 903K TEMPERATURE

Table 6.12

Experimental results of thermodynamic measurements for Bi and Sn at 903K

X_{Bi}	γ_{Bi}	a_{Bi}	$\Delta\bar{G}_{Bi}$ *[J/mol]*	X_{Sn}	γ_{Sn}	a_{Sn}	$\Delta\bar{G}_{Sn}$ *[J/mol]*
1,0	1,0	1,0	0	**0**	2,718	0	$-\infty$
0,9	1,090	0,971	-7,512	**0,1**	2,460	0,246	-10530
0,8	1,171	0,935	-488,56	**0,2**	2,226	0,445	-6079
0,7	1,243	0,869	-1046	**0,3**	2,014	0,604	-3785
0,6	1,315	0,789	-1779	**0,4**	1,822	0,728	-2373
0,5	1,376	0,687	-2808	**0,5**	1,649	0,824	-1444
0,4	1,477	0,591	-3949	**0,6**	1,492	0,895	-832,823
0,3	1,640	0,492	-5324	**0,7**	1,350	0,945	-424,704
0,2	1,997	0,399	-6898	**0,8**	1,221	0,976	-174,69
0,1	2,480	0,298	-9886	**0,9**	1,105	0,995	-37,632
0	3,123	0	$-\infty$	**1,0**	1,0	1,0	0

Table 6.13

Experimental results of thermodynamic measurements for Bi and Sn at 600K

X_{Bi}	*Calculated values [J/mol]*			*Magnus and Mannheimer*			X_{Sn}	*Calculated values [J/mol]*			*Magnus and Mannheimer*		
	γ_{Bi}	a_{Bi}	$\Delta\bar{G}_{Bi}$ *[J/mol]*	γ_{Bi}	a_{Bi}	$\Delta\bar{G}_{Bi}$ *[J/mol]*		γ_{Sn}	a_{Sn}	$\Delta\bar{G}_{Sn}$ *[J/mol]*	γ_{Sn}	a_{Sn}	$\Delta\bar{G}_{Sn}$ *[J/mol]*
1,0	1,0	1,0	0	1,0	1,0	0	**0**	1,28	0	$-\infty$	1,156	0	$-\infty$
0,9	1,01	0,909	-475,94	1,0	0,9	-525,58	**0,1**	1,25	0,125	-10370	1,159	0,116	-10750
0,8	1,011	0,809	-1057	1,002	0,802	-1101	**0,2**	1,19	0,238	-7161	1,145	0,229	-7353
0,7	1,012	0,708	-1723	1,009	0,706	-1737	**0,3**	1,15	0,346	-5294	1,122	0,337	-5426
0,6	1,031	0,619	-2393	1,021	0,613	-2441	**0,4**	1,12	0,448	-4005	1,097	0,439	-4107
0,5	1,032	0,516	-3301	1,039	0,519	-3272	**0,5**	1,09	0,545	-3028	1,075	0,537	-3102
0,4	1,057	0,423	-4292	1,065	0,426	-4257	**0,6**	1,068	0,641	-2218	1,053	0,632	-2289
0,3	1,111	0,333	-5485	1,104	0,331	-5515	**0,7**	1,046	0,732	-1556	1,033	0,723	-1618
0,2	1,194	0,239	-7140	1,16	0,232	-72,88	**0,8**	1,026	0,821	-983,873	1,016	0,813	-1033
0,1	1,259	0,126	-10330	1,241	0,124	-10410	**0,9**	1,014	0,913	-454,041	1,004	0,904	-503,495
0	1,328	0	$-\infty$	1,356	0	$-\infty$	**1,0**	1,0	1,0	0	1,0	1,0	0

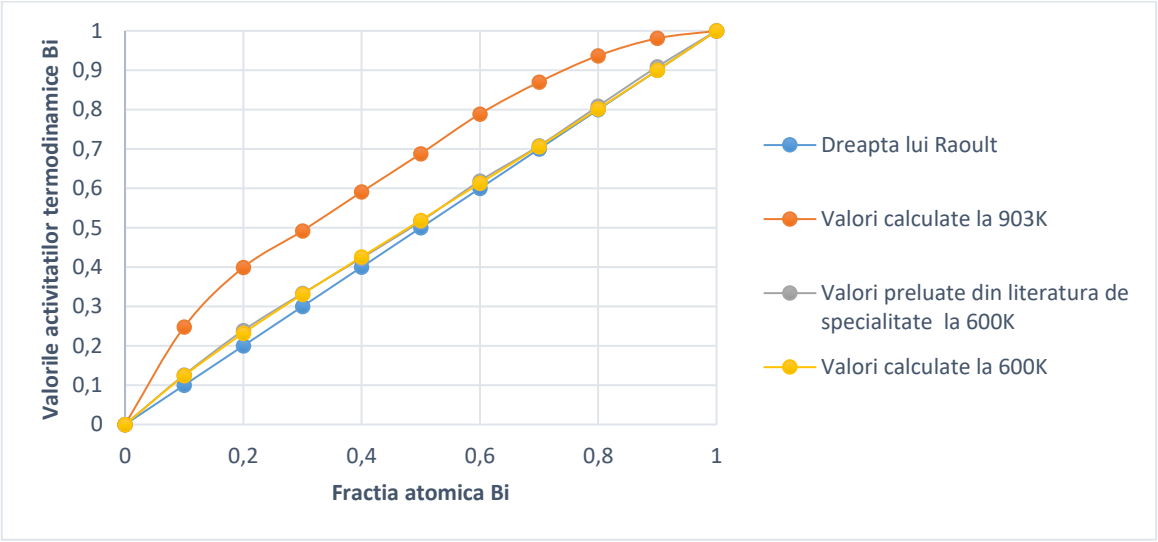

Figure 6.13 Variation of the thermodynamic activity of Bi as a function of atomic fraction in the Bi-Sn binary alloy at 903K and 600K experimental values and values from the literature

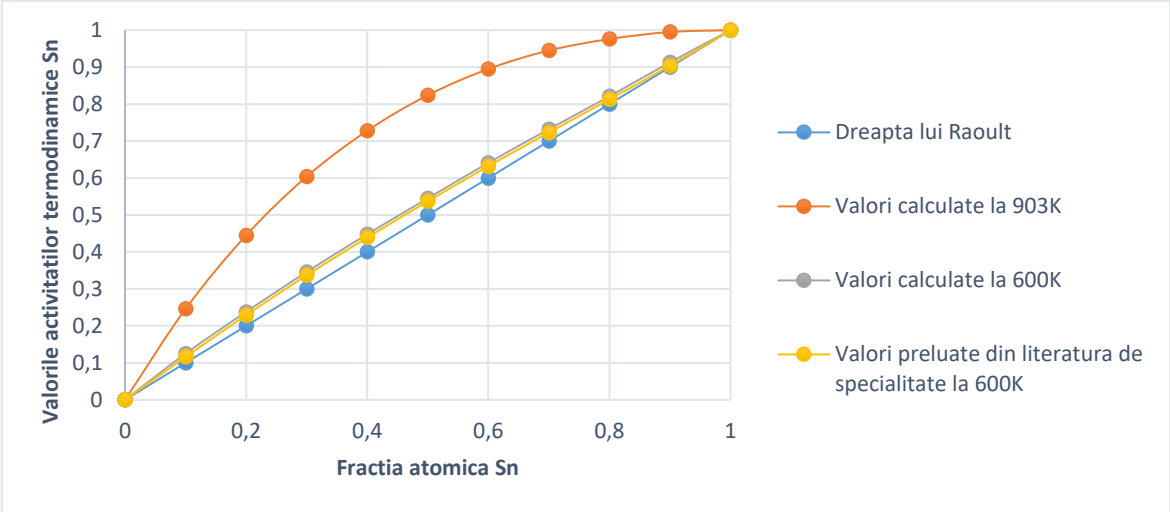

Figure 6.14 Variation of the thermodynamic activity of Sn as a function of the atomic fraction in the Bi-Sn binary alloy at 903K and 600K experimental values and values from the literature

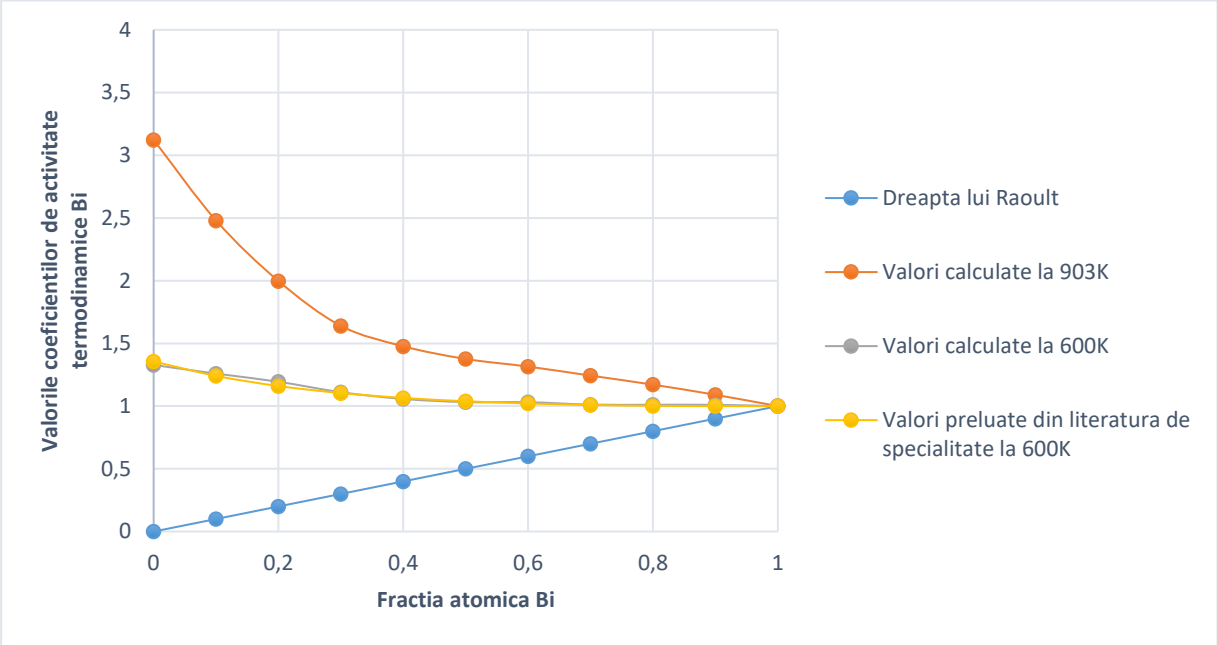

Figure 6.15 Variation of thermodynamic activity coefficients for Bi as a function of atomic fraction in Bi-Sn binary alloy at 903K and 600K experimental values and values calculated based on data from the literature

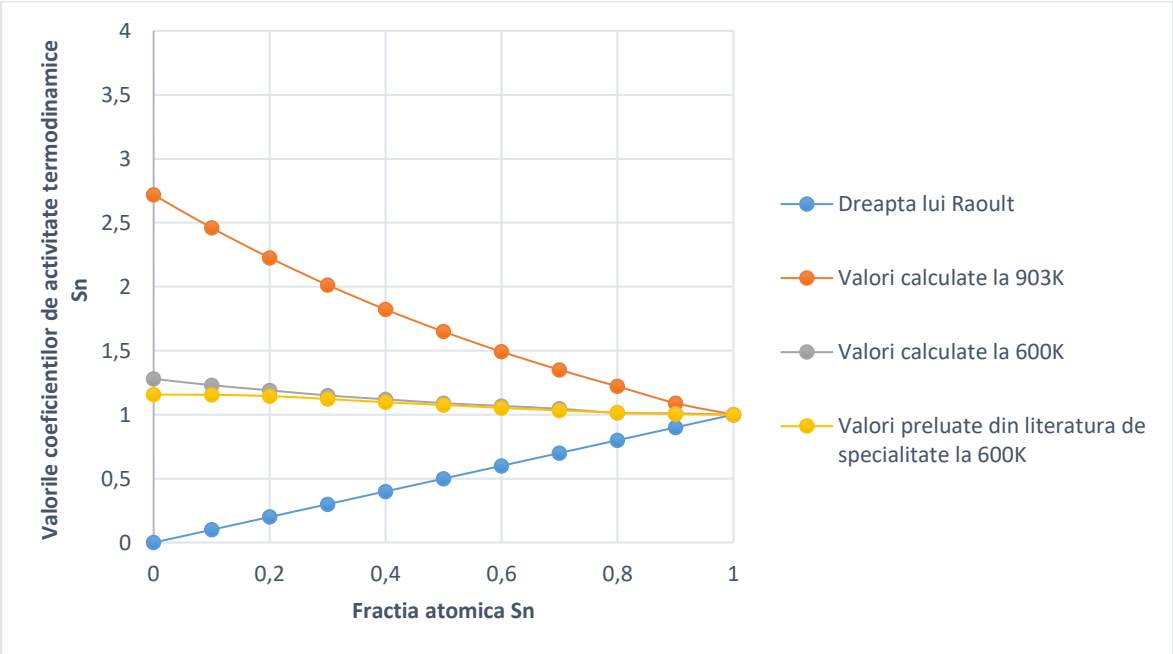

Figure 6.16 Variation of thermodynamic activity coefficients for Sn as a function of atomic fraction in Bi-Sn binary alloy at 903K and 600K experimental values and values calculated based on data from the literature

Table 6.14

Partially molar enthalpies of Bi and Sn at T = 600 K

X_{Bi}	$\Delta\overline{H}_{Bi}$ *[J/mol]*	$\Delta\overline{H}_{Sn}$ *[J/mol]*
0,0	$-6{,}093\cdot10^3$	$-5{,}812\cdot10^3$
0,1	$-3{,}389\cdot10^3$	$-2{,}593\cdot10^3$
0,2	$-1{,}188\cdot10^3$	$-1{,}188\cdot10^3$
0,3	$0{,}498\cdot10^3$	$0{,}117\cdot10^3$
0,4	$1{,}978\cdot10^3$	$2{,}270\cdot10^3$
0,5	$3{,}469\cdot10^3$	$4{,}365\cdot10^3$
0,6	$5{,}265\cdot10^3$	$6{,}244\cdot10^3$
0,7	$8{,}023\cdot10^3$	$8{,}045\cdot10^3$
0,8	$1{,}398\cdot10^4$	$9{,}724\cdot10^3$
0,9	$1{,}634\cdot10^4$	$1{,}118\cdot10^4$
1,0	*0*	*0*

-

Table 6.15

Partially molar enthalpies of Bi and Sn at T = 900 K

X_{Bi}	$\Delta\overline{H}_{Bi}$ *[J/mol]*	$\Delta\overline{H}_{Sn}$ *[J/mol]*
0,0	$-9{,}166\cdot10^3$	$-4{,}054\cdot10^3$
0,1	$-5{,}100\cdot10^3$	$0{,}302\cdot10^3$
0,2	$-1{,}788\cdot10^3$	$3{,}674\cdot10^3$
0,3	$0{,}751\cdot10^3$	$6{,}533\cdot10^3$
0,4	$2{,}977\cdot10^3$	$9{,}077\cdot10^3$
0,5	$5{,}217\cdot10^3$	$1{,}131\cdot10^3$
0,6	$7{,}911\cdot10^3$	$1{,}341\cdot10^3$
0,7	$1{,}207\cdot10^3$	$1{,}528\cdot10^3$
0,8	$2{,}104\cdot10^4$	$1{,}682\cdot10^3$
0,9	$2{,}459\cdot10^4$	$1{,}871\cdot10^4$
1,0	*0*	*0*

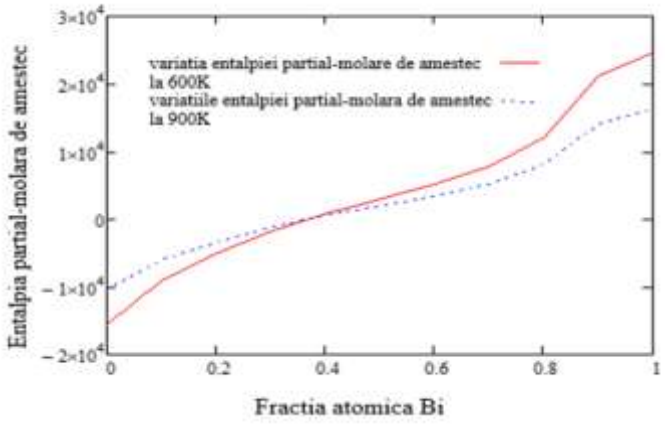

Figure 6.17 Variation of partial-molar enthalpies of mixture for Bi as a function of atomic fraction in Bi-Sn binary alloy at 903K and 600K experimental values and values calculated based on data from the literature

Table 6.16

Partially molar enthalpies of Bi and Sn at 903K

X_{Bi}	$\Delta\bar{S}_{Bi}$ [J/mol]	$\Delta\bar{S}_{Sn}$ [J/mol]
0,0	27,227	20,721
0,1	23,304	18,631
0,2	14,194	16,964
0,3	10,540	*15,047*
0,4	8,671	13,000
0,5	7,354	10,975
0,6	6,335	8,831
0,7	5,154	6,696
0,8	3,498	4,524
0,9	1,743	*2,245*
1,0	0	*0*

Table 6.17

Fully molar and fully molar free energies of excess at T = 600K

X_{Bi}	ΔG [J/mol]	ΔG^E [J/mol]
0,0	*0*	*0*
0,1	*-6425*	*-35620*
0,2	*-5802*	*-32060*
0,3	*-5292*	*-28590*
0,4	*-4906*	*-21990*
0,5	*-4679*	*-18920*
0,6	*-4672*	*-16060*
0,7	*-4946*	*-13490*
0,8	*-5674*	*-11370*
0,9	*-7157*	*-10000*
1,0	*0*	*0*

Table 6.18

Fully molar and fully molar free energies of excess at T = 903K

X_{Bi}	ΔG [J/mol]	ΔG^E [J/mol]
0,0	*0*	*0*
0,1	*-602*	*-9820*
0,2	*-1177*	*-11850*
0,3	*-1739*	*-14450*
0,4	*-2249*	*-17400*
0,5	*-2853*	*-20550*
0,6	*-3593*	*-23830*
0,7	*-4697*	*-27180*
0,8	*-6548*	*-30570*
0,9	*-10530*	*-33970*
1,0	*0*	*0*

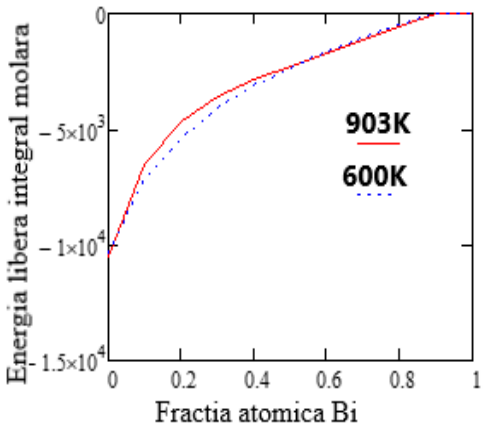

Figure 6.18 Variation of fully molar free energy as a function of atomic fraction in Bi-Sn binary alloy at 903K and 600K experimental values and values calculated based on data from the literature

Table 6.19

Fully molar and excess enthalpies of Bi and Sn at T = 600K

x_{Sb}	ΔH [*J/mol*]	ΔH^E [*J/mol*]
0,0	0	0
0,1	-19960	-18140
0,2	-11360	-14020
0,3	-8794	-11410
0,4	-6838	-9188
0,5	-5248	-7031
0,6	-3908	-4865
0,7	-2769	-2791
0,8	-1756	-870
0,9	-817	736
1,0	0	0

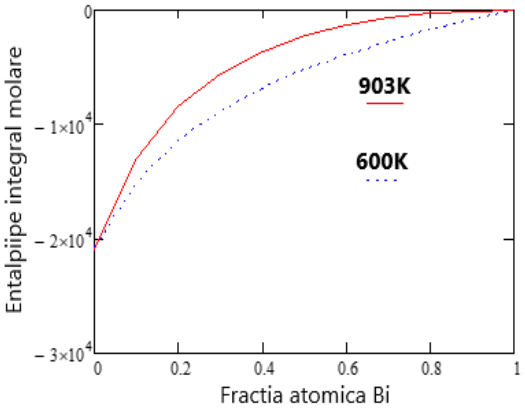

Figure. 6.19 Variation of the integral molar enthalpy according to the atomic fraction in the Bi-Sn binary alloy at 903K and 600K experimental values and calculated values based on data from the literature

Table 6.20

Integrally molar and excess enthalpies of Bi and Sn at T = 903K

x_{Sb}	ΔH [*J/mol*]	ΔH^E [*J/mol*]
0,0	0	0
0,1	-13050	-17130
0,2	-8486	-11370
0,3	-5593	-8019
0,4	-3628	-5280
0,5	-2278	-2672
0,6	-1342	-95
0,7	-698	2391
0,8	-295	4616
0,9	-68	6381
1,0	0	0

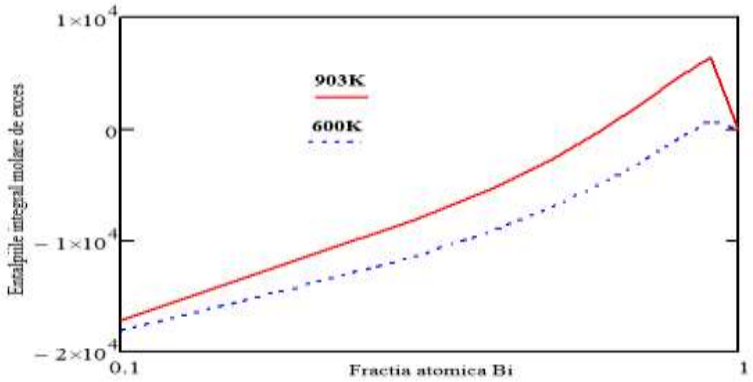

Figure 6.20 Variation of the integral molar enthalpy of excess depending on the atomic fraction in the binary alloy Bi-Sn at 903K and 600K experimental values and values calculated based on data from the literature

Table 6.21

Fully molar and fully molar excess entropies at T = 600K

x_{Sb}	ΔS [*J/mol*]	ΔS^E [*J/mol*]
0,0	0	0
0,1	-1,189	1,514
0,2	0,922	5,082
0,3	3,850	8,929
0,4	6,186	11,781
0,5	7,469	13,232
0,6	7,632	13,228
0,7	6,726	11,805
0,8	4,890	9,051
0,9	2,606	5,309
1,0	0	0

Table 6.22

Fully molar and fully molar excess entropies at T = 903K

x_{Sb}	ΔS [*J/mol*]	ΔS^{E} [*J/mol*]
0,0	0	0
0,1	-1,189	1,514
0,2	0,922	5,082
0,3	3,85	8,929
0,4	6,186	11,781
0,5	7,469	13,232
0,6	7,632	13,228
0,7	6,726	11,805
0,8	4,89	9,051
0,9	2,606	5,309
1,0	0	0

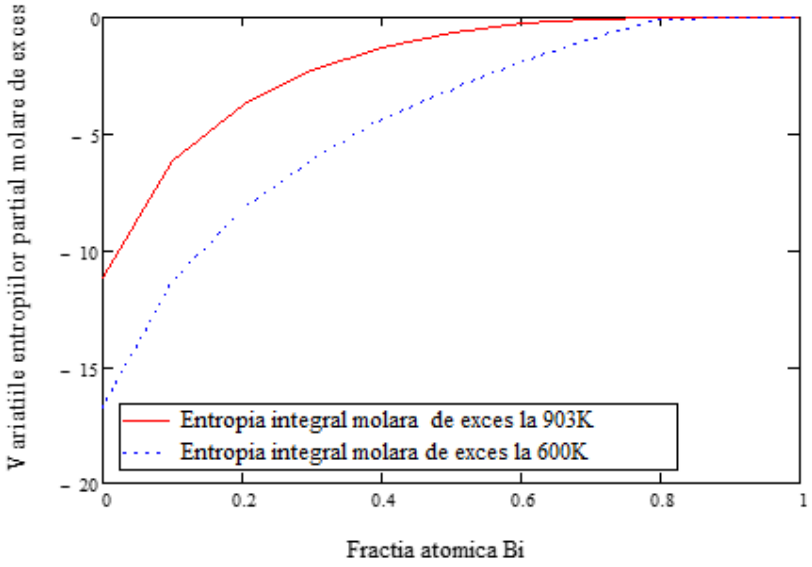

Figure 6.21 Variation of integral molar entropies of excess as a function of atomic fraction in Bi-Sn binary alloy at 903K and 600K experimental values and values calculated based on data from the literature

6.4. THERMODYNAMIC MODELING WITH THE HELP OF THE EMPIRICAL MARGULES MODEL OF THE Bi-Sn BINARY ALLOY SYSTEM

Table 6.23

Experimental values and calculated values of activity coefficients at 600K using the MARGULES model. (Annex 9).

$X_{Bi(600)}$	*0,0*	*0,1*	*0,2*	*0,3*	*0,4*	*0,5*	*0,6*	*0,7*	*0,8*	*0,9*	*1,0*
Valorile experimentale											
γ_{Bi}	*1,328*	*1,256*	*1,194*	*1,110*	*1,060*	*1,032*	*1,023*	*1,012*	*1,011*	*1,01*	*1,000*
γ_{Sn}	*1,000*	*1,014*	*1,026*	*1,046*	*1,068*	*1,090*	*1,120*	*1,150*	*1,190*	*1,250*	*1,280*

Valorile calculate											
γ_{cBi}	*1,327*	*1,261*	*1,185*	*1,115*	*1,062*	*1,031*	*1,018*	*1,015*	*1,013*	*1,006*	*1,000*
γ_{cSn}	*1,000*	*1,008*	*1,026*	*1,048*	*1,069*	*1,091*	*1,116*	*1,150*	*1,195*	*1,246*	*1,281*

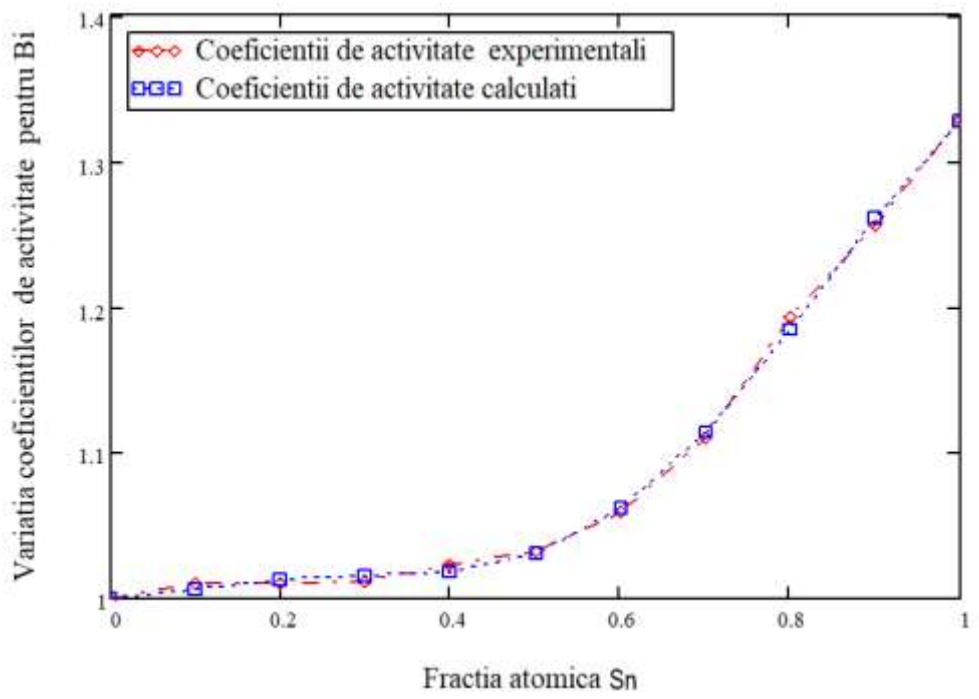

Figure.6.22. Bi activity coefficient values, experimental values and values calculated using the MARGULES model at 600K.

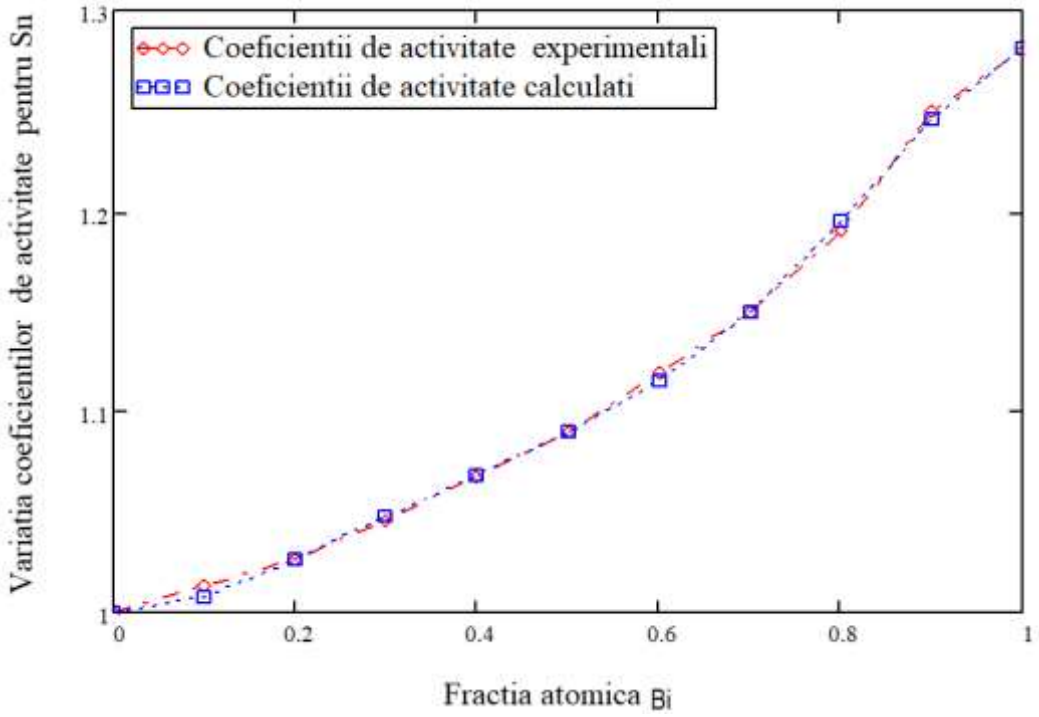

Figure.6.23. Sn activity coefficient values, experimental values and values calculated using the MARGULES model at 600K.

Table 6.24

Experimental values and calculated values of activity coefficients at 600K using the MARGULES model. (Appendix 9).

$X_{Bi(903)}$	*0,0*	*0,1*	*0,2*	*0,3*	*0,4*	*0,5*	*0,6*	*0,7*	*0,8*	*0,9*	*1,0*
Experimental values											
γ_{Bi}	*3,623*	*2,980*	*1,995*	*1,640*	*1,475*	*1,374*	*1,311*	*1,241*	*1,160*	*1,080*	*1,000*
γ_{Sn}	*1,000*	*1,105*	*1,221*	*1,350*	*1,492*	*1,649*	*1,822*	*2,014*	*2,226*	*2,460*	*2,718*
Calculated values											
γ_{cBi}	*3,647*	*2,892*	*2,081*	*1,630*	*1,438*	*1,372*	*1,332*	*1,258*	*1,148*	*1,045*	*1,000*
γ_{cSn}	*1,000*	*1,077*	*1,222*	*1,365*	*1,496*	*1,637*	*1,813*	*2,023*	*2,240*	*2,444*	*2,723*

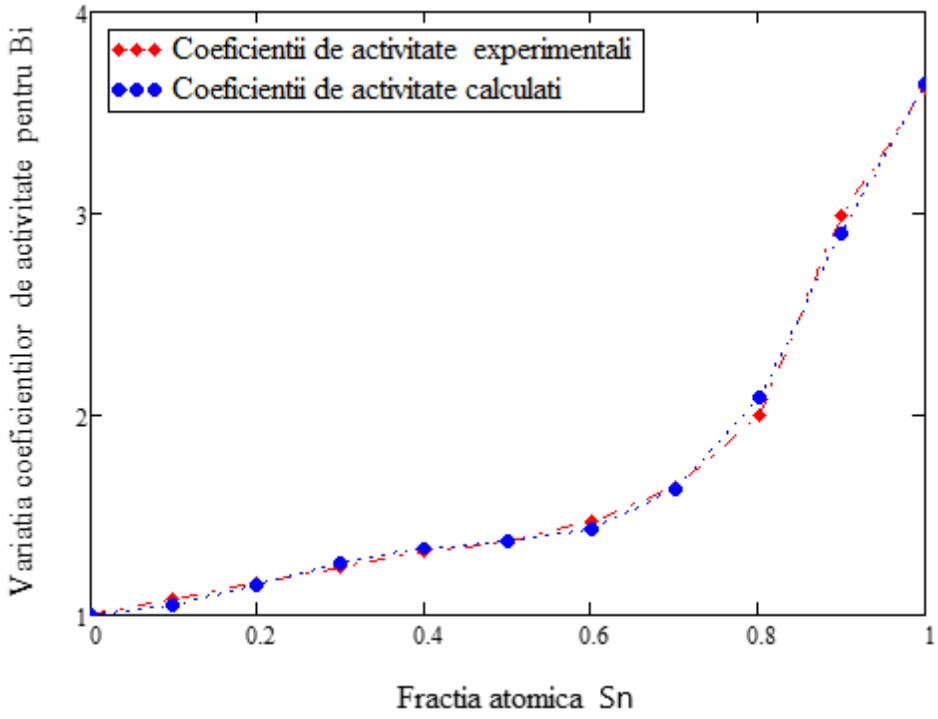

Figure.6.24. Bi activity coefficient values, experimental values and values calculated using the MARGULES model at 903K.

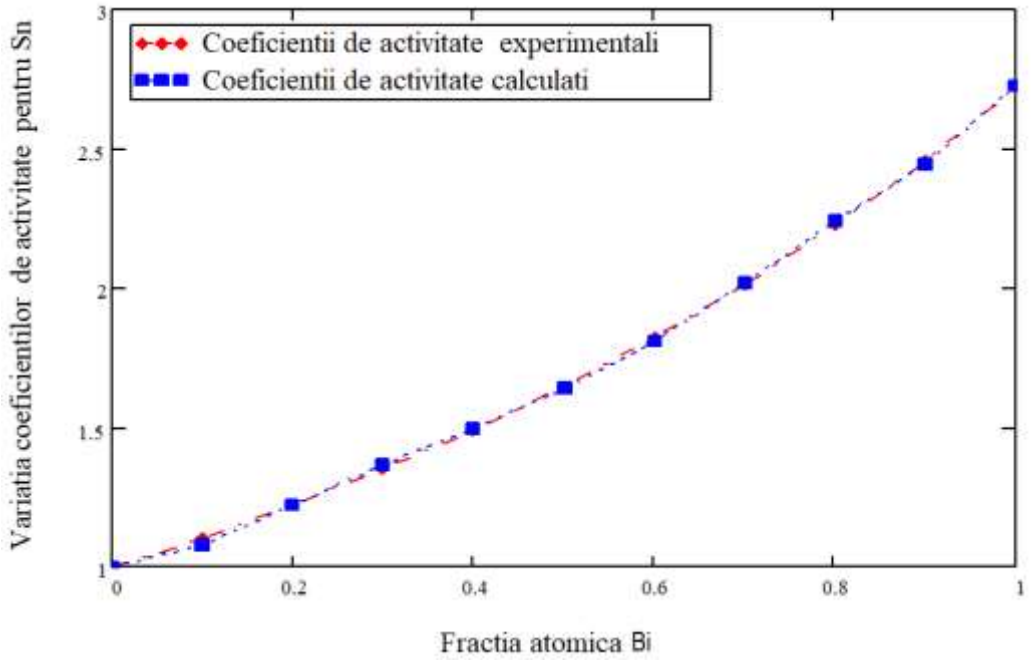

Figure.6.5. Sn activity coefficient values, experimental values and values calculated using the MARGULES model at 903K..

6.5. THERMODYNAMIC MODELING WITH THE HELP OF THE THEORETICAL MODEL, THE MODEL OF THE SUBSUBREGULAR SOLUTION OF THE BINARY ALLOY SYSTEM Bi-Sn

Table 6.25

Experimental values and calculated values of activity coefficients at 600K using the subsubregular solution model. (Annex 10)

$X_{Bi(600)}$	0,0	0,1	0,2	0,3	0,4	0,5	0,6	0,7	0,8	0,9	1,0
Experimental values											
γ_{Bi}	1,328	1,256	1,194	1,110	1,060	1,032	1,023	1,012	1,011	1,01	1,000
γ_{Sn}	1,000	1,014	1,026	1,046	1,068	1,090	1,120	1,150	1,190	1,250	1,280
Calculated values											
γ_{cBi}	1,335	1,250	1,178	1,119	1,073	1,039	1,017	1,005	1,000	1,000	1,000
γ_{cSn}	1,000	1,007	1,024	1,048	1,075	1,104	1,133	1,164	1,198	1,240	1,294

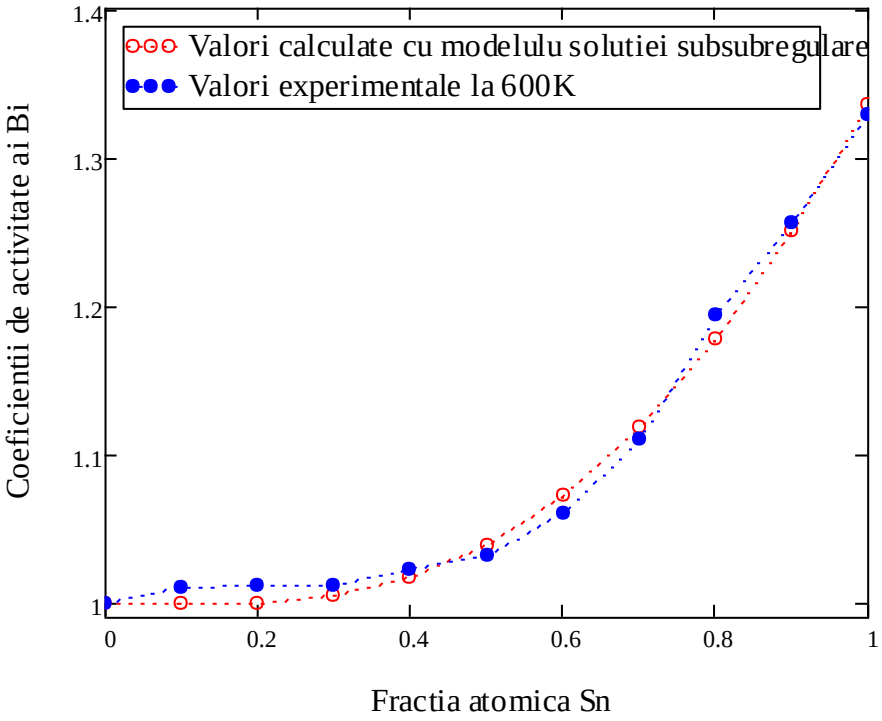

Figure.6.26. Values of Bi activity coefficients, experimental values and values calculated using the model of subsubregular solutions at a temperature of 600K.

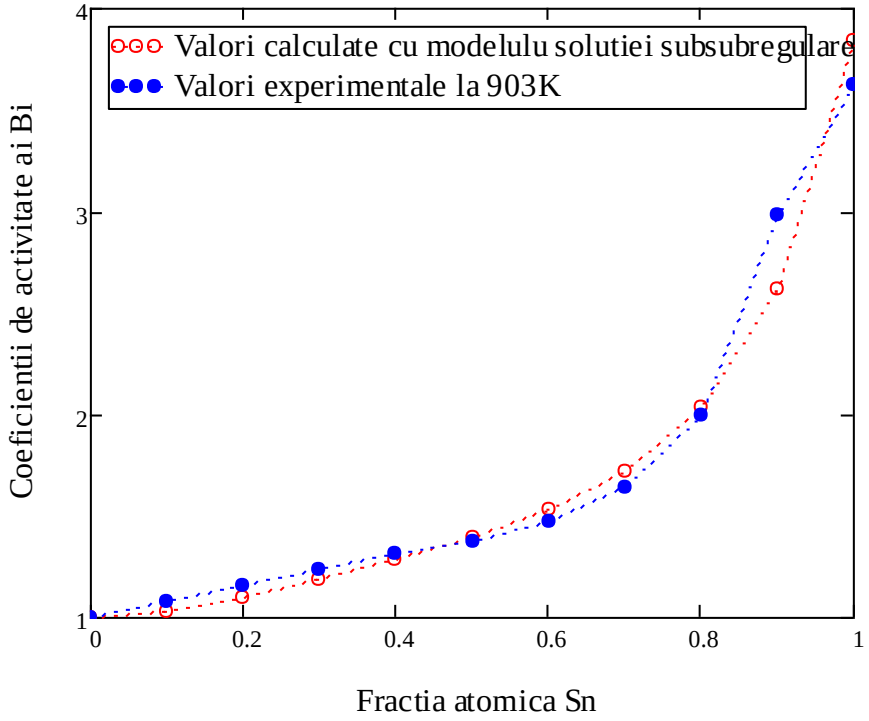

Figure.6.27. Values of Bi activity coefficients, experimental values and values calculated using the model of subsubregular solutions at a temperature of 600K.

Table 6.26

Experimental values and calculated values of activity coefficients at 903K using the subsubregular solution model. (Annex 10)

$X_{Bi(903)}$	0,0	0,1	0,2	0,3	0,4	0,5	0,6	0,7	0,8	0,9	1,0
Experimental values											
γ_{Bi}	3,623	2,980	1,995	1,640	1,475	1,374	1,311	1,241	1,160	1,080	1,000
γ_{Sn}	1,000	1,105	1,221	1,350	1,492	1,649	1,822	2,014	2,226	2,460	2,718
Calculated values											
γ_{cBi}	3,846	2,619	2,034	1,721	1,553	1,399	1,287	1,186	1,096	1,028	1,000
γ_{cSn}	1,000	1,037	1,140	1,300	1,511	1,761	2,031	2,294	2,517	2,666	2,718

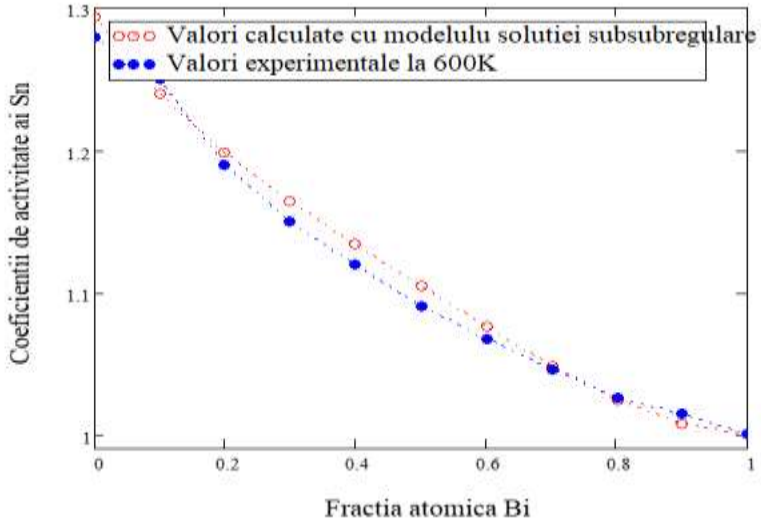

Figure.6.28. Values of Sn activity coefficients, experimental values and values calculated using the model of subsubregular solutions at a temperature of 600K.

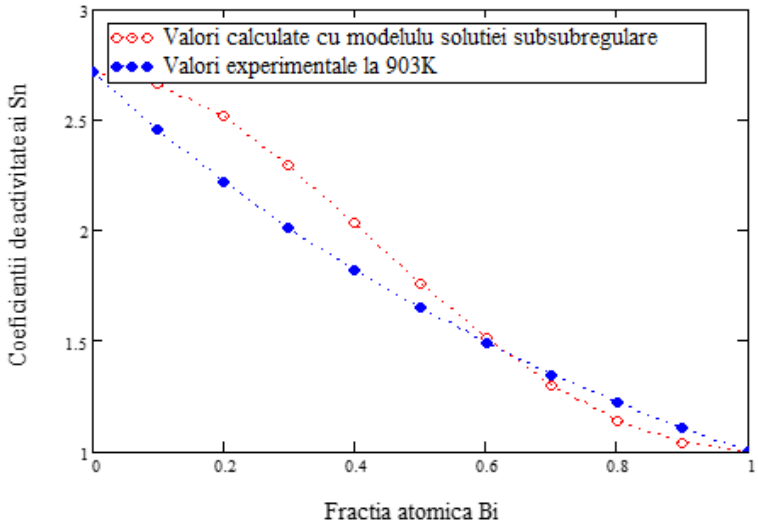

Figure.6.28. Values of Sn activity coefficients, experimental values and values calculated using the model of subsubregular solutions at a temperature of 903K.

6.6 ELABORATION AND PHYSICO-CHEMICAL AND STRUCTURAL CHARACTERIZATION OF THE Bi-Sn ALLOY

6.6.1 WORKING METHOD USED IN ELABORATION OF THE ALLOY

In the elaboration of the binary alloy Sn-Bi we used Bi of purity 99.6%, and Sn purity 99.8%. Two sets of samples were obtained, an alloy sample made in the quartz cell where the electromotive voltage was measured at 903K in the form of a bar (3x4cm) and a sample made later in graphite crucible with three different alloy compositions.

The second set of samples was melted and poured into crucibles and graphite molds. NH_4Cl (refined ammonium chloride) was used as protection flow / coating of the metal bath from the action of oxidizing gases inside the furnace. The elaboration process was continued by the preparation of materials and raw materials (primary preparation and preparation for loading). Through the primary preparation, the qualitative and quantitative verification of the raw materials and auxiliary materials used was performed. During the same stage we dosed, dimensioned and weighed (electronic balance) the raw materials.

6.6.2 ANALYSIS BY OPTICAL MICROSCOPY

Samples from conventionally cast Bi-Sn binary alloys were characterized by analysis of optical microscopy with Optika optical microscope model B383 MET, equipped with digital camera and software for image processing.

Prior to microscopic study, samples were prepared metallographically to highlight the structure of the material obtained. The images below show the microstructures of the cast alloys, at different magnifications of the objective. The micrograph shows the modification of the microstructure of each sample as the percentage composition of bismuth is varied.

6.6.3 STRUCTURAL ANALYSIS BY XRD- ED (P) -XRFS

The most efficient approach to the elemental and structural characterization of Bi-Sn alloys can be achieved using X-ray Fluorescence Spectrometry (XRFS X-ray Fluorescent Spectromety) and X-ray Diffractometry as these are instrumental techniques which requires minimal preparation of the samples to be analyzed and provides a wide range of information on the elemental and phasic compositions of the investigated samples.

6.6.3.1 EXPERIMENTAL RESULTS

Three representative alloys obtained Bi25-Sn75, Bi50-Sn50 and Bi75-Sn25 were investigated. Sample code 1 (Bi-Sn75) provided 3 XRF spectra (Fig. 6) obtained by secondary scattering of X-ray of Rh on targets in Al_2O_3-blue curve-; Mo-red curve and HOPG-magenta curve. It can be seen that the fluorescence lines of Sn and Bi are dominant.

7. CONCLUSIONS

The doctoral thesis aimed to carry out experimental research on solder alloys used in key fields such as electronics and electrical engineering. The importance of solder alloys is reflected in the high market demand based mainly on solder alloys without toxic elements in their composition. The aim is to eliminate especially lead known as a very toxic element, practically a metabolic poison affecting the central nervous system, immunity, reproducibility and the cardiovascular system. This toxic element produces undesirable and irreversible effects on the whole environment. In a World Health Organization ranking, lead is found in the top of hazardous chemicals.

- ✓ Based on the importance of these types of alloys in the industry, I chose to study Bi and Sn-based solder alloys because they have far superior properties to pure alloy metals. Studying the literature, I came to the conclusion that there is a very limited number of experimental data and few studies performed on a limited range of temperatures and concentrations. Very old experimental data, working technique, outdated equipment and few thermodynamic data at certain temperatures required new thermodynamic experiments.
- ✓ In this research paper on the thermodynamics of Bi-Sn binary alloys I used the method of measuring electromotive voltage, a precise, safe, and reproducible method.
- ✓ I performed experiments at working temperatures for which data already existed in the literature (600K). Uncertainty values were calculated with the corresponding confidence level. Experiments and calculations have shown that the method is safe and reproducible.
- ✓ Also for a better interpretation of the experimental data we have developed in this paper a program called "binary thermodynamic calculation - CTB" using the Netbeans IDE environment version 8.02 and the Java programming language. This program was born out of the desire to calculate with high accuracy the imported thermodynamic functions and to compare them with those already known.
- ✓ The cell used during the experiment came with a previous improvement, namely the multiple holes ensuring a better electrolyte circuit through the two semi-elements.
- ✓ We calculated the values of the thermodynamic activities, the activity coefficients, for Sn and Bi in the binary alloy Bi-Sn at the temperature of 600K and we reported them to the right of Raoult. In both cases, the values obtained are above Raoult's line, so they show positive deviations from ideality. Experimental values are close to unity in the whole range of concentrations and values in the literature, which indicates an approach to ideal solutions. The values obtained in this work differ from those already existing because the work technique and equipment has known over the years a continuous improvement.
- ✓ We performed calculations of the partially-molar enthalpies of the mixture, the partially molar entropies of the mixture, the free energy of the molar and the molar of excess, the enthalpies of the molar and the molar of the excess 600K. After their graphical representation, it was concluded that the data obtained are in accordance with the data in the literature with differences in values that fall from the work technique performance.
- ✓ We obtained the temperature dependencies of the thermodynamic quantities enthalpies, entropies and free energies Gibbs for both Bi and Sn at the temperature of 600K.
- ✓ Making an analysis and a comparison of the known empirical models we chose the most exact model, namely the Margules model and we thermodynamically modeled this binary alloy. The conclusion was that Sn and Bi are elements with similar behavior and

that the experimental and calculated values are correct. The graphical representation shows an approximation of the experimental values to those of the model, some of the values being identical. Both the Bi and Sn properties are accurately described by the Margules model and certify the correctness of the experiments as well as the preliminary calculations.

- ✓ Making an analysis and a comparison of the known theoretical models we chose the model of the subsubregular solution and we thermodynamically modeled this binary alloy. The conclusion was that Sn and Bi are elements with similar behavior but that the model better describes the properties of bismuth. And in this case the graphical representation shows an approximation of the experimental values to those of the model, more precise being those of bismuth. From the thermodynamically point of view, the two elements behave similarly, the obtained models making a very good description of the thermodynamic properties of bismuth and tin; it is found, however, that the tested models are more accurate in the case of bismuth.
- ✓ We performed experiments at working temperatures which are not found in the literature (903K). And for this temperature, the uncertainty values were calculated with the corresponding confidence level, which certified us that the experiments and calculations performed were correct.
- ✓ We calculated the thermodynamic activities, the activity coefficients, the thermodynamic functions of temperature, enthalpy, entropy, free energy as well as the partial-molar and excess free energies at the temperature of 903K. At this temperature no data are known in the literature. The values of the activities and those of the coefficients of thermodynamic activity as a function of the atomic fraction were reported to Raoult's right. The values obtained are above Raoult's line, so they show positive deviations from ideality.
- ✓ We obtained the temperature dependencies of the thermodynamic quantities enthalpies, entropies and Gibbs free energies for both Bi and Sn at 903K.
- ✓ The values obtained at the temperature of 903K were compared with those calculated at 600K and with the values already existing. All these values were plotted and it was observed that the values follow the same trends, the data agree and that the experiment was performed correctly.
- ✓ A general conclusion is that the thermodynamic functions obtained for the thermodynamic characterization of Bi-Sn binary alloy systems, allow the coverage by calculation of any point of interest temperature-concentration, with a very high precision.
- ✓ We developed (casting) and investigated three types of alloys 1. Bi25 -Sn75, 2. Bi50-Sn50 and 3. Bi75-Sn25 by optical microscopy. Individual microstructural variations of the samples were observed depending on the amount of bismuth. Sn-based matrix structures, Bi-based matrix structures, balanced structures with a large amount of intermetallic constituents without conglomerates and / or clusters causing heterogeneity in the chemical composition, uniformly distributed metal phases were obtained, and even the formation of compounds with polyhedral or tetragonal shapes.
- ✓ The three types of alloys were analyzed using the X-ray diffractometer. From the analyzes performed it was confirmed to obtain the alloy provided with very low tolerances for tin and bismuth. The first sample provided three XRF spectra dominating the fluorescence lines of bismuth and tin. From the semi-quantitative phase analysis it shows that the sample contains mainly 2 phases rich in Sn in a proportion of about 90% and 9% Bi segregated. Percentages of Bi (25%) are found in two states: diffused and segregated in Sn with the formation of a Bi-Sn eutectic.

- ✓ Sample two provided fluorescence spectra with more intense lines in the low energy area of the spectra due to the increase of the Bi weight in the alloy. The diffractometric investigations performed on this sample show an increase in the intensities of the diffraction lines related to the metallic Bi phase and a decrease in the line intensities of the compound Sn0.95 -Bi0.5 which corresponds to the state of the designed alloy.
- ✓ The elemental composition of sample three is very close in value to the designed composition of the standard. The identified residual elements can be attributed to impurities in precursors or to artifacts such as compton scattering of Sn and Bi fluorescence specific photons. Diffractometric analysis shows the prevalence of Bi in the metallic state and the formation of the compound Sn0.95Bi0.5 and traces of metallic Sn.
- ✓ Making a comparative analysis of the diffractometric results, the conclusion is that the tested alloys have been elaborated correctly and are convergent with the EDP-XRD analyzes presented previously.

7.1. ORIGINAL CONTRIBUTIONS

- Extensive study of the literature on lead-free solder alloys.
- Updated study of thermodynamic modeling as well as the calculation of thermodynamic functions.
- Experimental measurements made at a temperature of 600K for which they are given in the literature.
- Experimental measurements performed at a temperature of 903K for which they are not given in the literature.
- Calculation of activities, activity coefficients, partially molar thermodynamic properties, integral-molar thermodynamic properties of mixture and excess and the calculation of Gibbs free energies for the temperature of 600K.
- Obtaining the temperature dependencies of the thermodynamic quantities: enthalpies, entropies and Gibbs free energies for Bi and Sn at 600K.
- Calculation of activities, activity coefficients, partial thermodynamic properties molar, integral-molar thermodynamic properties of mixture and excess and calculation Gibbs free energy for 903K temperature.
- Obtaining the temperature dependencies of the thermodynamic quantities: enthalpies, entropies and Gibbs free energies for Bi and Sn at the temperature of 903K.
- Modeling the Bi-Sn binary system using the Margues model.
- Modeling the Bi-Sn binary system using the subsubregular solution model.
- Elaboration, investigation and interpretation of the obtained results of the three types of alloys 1.Bi25-Sn75, 2.Bi50-Sn50 and 3.Bi75-Sn25 by microscopy optics.
- Diffractographic analysis and interpretation of the results obtained on the three types of alloys.
- Development of a program "binary thermodynamic calculation - CTB" that can be used for any calculation basis.

BIBLIOGRAPHY

[1*].P. Suksongkarm, S. Rojananan, S. Rojananan, Bismuth Formation in Lead-Free Cu–Zn–Si Yellow Brass with Various Bismuth–Tin Alloy Additions,* Mater. Trans. 58 (12) pp.1754–1760, (2017).
[2].*S. Knott, Z. Li, C.H. Wang, and A. Mikula,* Measurement of Activity of Indium in Liquid Bi-In-Sn Alloys by EMF Method Metall. Mater. Trans. A 41, 3130 (2010).
[3].*Y.Dahan, G.Makov, R.Z.Shneck,* Nanometric size dependent phase diagram of Bi-Sn, Calphad Volume 53, Pages 136-145,(2016).
[4].*Z. Guo, W. Yuan, M. Hindler, A. Mikula,* Properties and Microstructures of Sn-Bi-X Lead-Free Solders *J. Chem.* Thermodynamics 48, pp.201–206, (2012).
[5].*N. Asryan, A. Mikula,* Thermodynamic properties of Bi–Sn melts Inorg. Mater., 40(4),pp. 457–461 (2004).
[6].*A.Yazawa, T. Kawashima, K. Itagaki,* Thermodynamics of liquid Pb–In–Sn alloys determined by vapour pressure measurements, J. Japan Inst. Metals 32 , pp.1281–1287 (1968).
[7].*C.Yang, S. Zhou, S. Lin, H.* Nishikawa, Sn-3.0Ag-0.5Cu/Sn-58Bi composite solder joint assembled using a low-temperature reflow process for PoP technology, Journals Materials Volume 12 Issue 4, (2019).
[8].*D.R. Frear,J. R. Michael, P. F. Hlava* ,Analysis of the reaction between 60Sn-40Pb solder with a Pd-Pt-Ag-Cu-Au alloy, Journal of Electronic MaterialsVolume 22 Issue 2 pp 185–194 (1993).
[9].*I.Manasijević, L. Balanović, T.H. Grgurić, D. Minić, M. Gorgievski*, Study of Microstructure and Thermal Properties of the Low Melting Bi-In-Sn Eutectic Alloys, Mat. Res. 21 (6) pp.1–8, (2018).
[10].*R.Hultgen,* Ed., Selected values of the thermodynamic properties of binary alloys, ASM International, Materials Park, OH, (1973).
[11]. *P. F. Hlava D.R. Frear,J. R. Michael,* ,Analysis of the reaction between 50Sn-60Pb solder with a Pd-Pt-Ag-Cu-Au alloy , Journal of Electronic MaterialsVolume 22 Issue 2 pp 200–208 (1994).
[12]. *E. Niculescu, G. Iacob, F. Niculescu,* et al., Experimental Determination of the Activities of Liquid Bi-Sn Alloys , Journal of Phase Equilibria Diff, vol. 42, nr. 2, pg 278-289, (2021).
[13].*R Hultgren,. s.a*. Selected values of the thermodynamic properties of the elements, Metals Park, Ohio, ASM, (1990).
[14].*R.,Hultgren,* s.a. Selected values of the thermodynamic properties of binary alloys, Metals Park, Ohio, ASM, (1991).
[15]. *I. Barin,*. Thermochemical data of pure substances. Weinheim, VCH, 1989, (1993).
[16]. *** ASM Handbook. V.3. Alloy phase diagrams. Materials Park, Ohio, ASM, (1990).
[17]. *A. Podgornik, R. Bhargava,* Rudarsko-Met. Zbornik 4, pp.357–362, (1960).
[18]. *M. Hansen and K. Anderko,* Constitution of Binary Alloys, (New York: McGraw-Hill, (1958).
[19]. *C. Wagner, G. Englehardt,* Z. Physik. Chem. 159A, pp. 241–267 (1932).
[20].*T.B Massalski* et al (Eds) Binary alloy phase diagrams. V.1-3, Metals Park, Ohio, ASM, International, (1990).

[21]. *Landolt-Börnstein*. Numerical data and functional relationships in science and technology. Group IV. Vol.5.Phase equilibria, crystallographic and thermodynamic data of binary alloys. Berlin, (1992).
[22].*Z. Moser, W. Gasior, J. Pstrus* Surface tension measurements of the Bi-Sn and Sn-Bi-Ag liquid alloys, Journal of Electronic Materials v*olume 30, pages1104–1111 (2001)* Chemistry, 5th ed., W.H. Freeman and co., NY, (1994).
[23].*C. Yang, F. Chen, W. Gierlotka,* et al.*,* Thermodynamic properties and phase equilibria of Sn–Bi–Zn ternary alloys,Mater. Chem. Phys. 112, 94 (2008).
[24]. *SH Wang, TS Chin, CF Yang, SW Chen*. Pb-free solder-alloy based on Sn–Zn–Bi with the addition of germanium Journal of Alloys and Compounds Volume 497, Issues 1–2, Pages 428-431(2010).
[25].*I. Sanjuán, L. García-Cruz,* Bi–Sn nanoparticles for electrochemical denitrification: activity and selectivity towards N2 formation, Electrochimica Acta Volume 340, 20 (2020).
[26].*E.F. Kleijn, S.C.S. Lai,* M.T.M. Koper, P.R. Unwin Electrochemistry of nanoparticles Angew. Chem. Int. Ed., 53 pp. 3558-3586 (2014).
[27].*J. Vizdal, M.H. Braga, A. Kroupa, K.W* et al., Calphad 31, 438 (2007).
[28]. *M.H. Braga, J. Vizdal, A. Kroupa,*et al, Thermodynamic assessment of the Bi–Sn–Zn System, Calphad 31, 468 (2007).
[29].*D Giuranno, R Novakovic*, Journal of Materials Science Surface and transport properties of liquid Bi–Sn alloys, Materials in Electronics Volume 31, pages 5533–5545 (2020).
[30].*F.E. Witting, F. Huber,* Z. Physik. Chem. Frankfurt, 18, pp.330–347 (1958).
[31].*J.Vizdal, M.H. Braga, A. Kroupa,* et al., *Thermodynamic Assessment Of The Bi-In-Zn System*, Calphad 31, pp.438–448 (2007).
[32]. G. *Zhongnan , Y. Wenxia , M. Hindler, and Adolf Mikula,* Thermodynamic properties of liquid Au–Bi–Sn alloys, J Chem Thermodyn. 2012 May; 48(6): 201–206. (2012).
[33].*Han Gyeol Kim, Joonho Lee, Guy Makov,* Thermodynamic Calculation of Bi–Sn Alloy Phase Diagram Under Pressure with Advanced Density Measurements Metals and Materials International , Issue 5(2020).
[34].*D.Fang. X.Chang, ,G.H. .X.Ye, H.Wua,* et al., Synthesis and melting behaviour of Bi, Sn and Sn–Bi nanostructured alloy,Vacuum Volume 174, (2020).
[35].*B.W. Dong, J.C. Jie, X.X. Yao* et al.*, Chen,* Effect of Sn addition on morphology evolution of secondary phase in hypomonotectic Cu-Pb-Sn alloy during solidification,Journal of Alloys and Compounds,Volume 791, pp 936-946, (2019).
[36].*C.T. Wang, Y. He, T.G. Langdon,* The significance of strain weakening and self-annealing in a superplastic Bi–Sn eutectic alloy processed by high-pressure torsion,Acta Materialia, Volume 185, pp. 245-256, (2020).
[37].*A Dobosz, T Gancarz,* Reference Data for the Density, Viscosity, and Surface Tension of Liquid Al–Zn, Ag–Sn, Bi–Sn, Cu–Sn, and Sn–Zn Eutectic Alloys, Journal of Physical and Chemical Reference Data, Volume 47, Issue 1, (2018).
[38].*M.R. Kumar, S.Mohan, C.K. Behera,* Thermodynamic accessment experimentally on Bi-Sn System by Calorimeter ,Materials Today: Proceedings Volume 5, Issue 14, Part 2, Pages 27777-27785, (2018).